



**Advanced Multicomponent
Seismic Software**

**Analysis of seismic data recorded in September 2025
by network C8 (stations SV1S-SV5S)
at Aquistore test site**

Report AQ-2025-09-IM

December 09, 2025

Igor Morozov

igor.morozov@usask.ca

Contents

1. Station performance.....	3
Data recovery.....	3
2. Data quality.....	7
3. Processing procedure and parameters.....	9
4. Seismic event detection.....	10
Automatic detections.....	10
Event bulletins.....	11
Teleseismic events (class 1).....	12
Regional events (class 2).....	15
Local events (classes 3 and 4).....	15
Possible mine blasts at the Estevan mine (class 3a).....	15
Events related to mining operations (class 3b).....	19
Events in array proximity (classes 4a and 4b).....	24
5. SEGY files.....	26
6. Conclusions and recommendations.....	26

1. Station performance

Station performance for September 2025 is summarized in Figure 1, and state-of-health data are shown in Figure 2. The only significant technical issue (not visible in these Figures but noticeable seen in amplitude plots and data records below) was a poor performance of sensors at station SV3S.

The Missing uptime log on September 1-14 for station SV4S and state-of-health data for SV2S were due to replacing the modems.

Data recovery

Data recovery was nearly 100% from all channels (Figure 1).

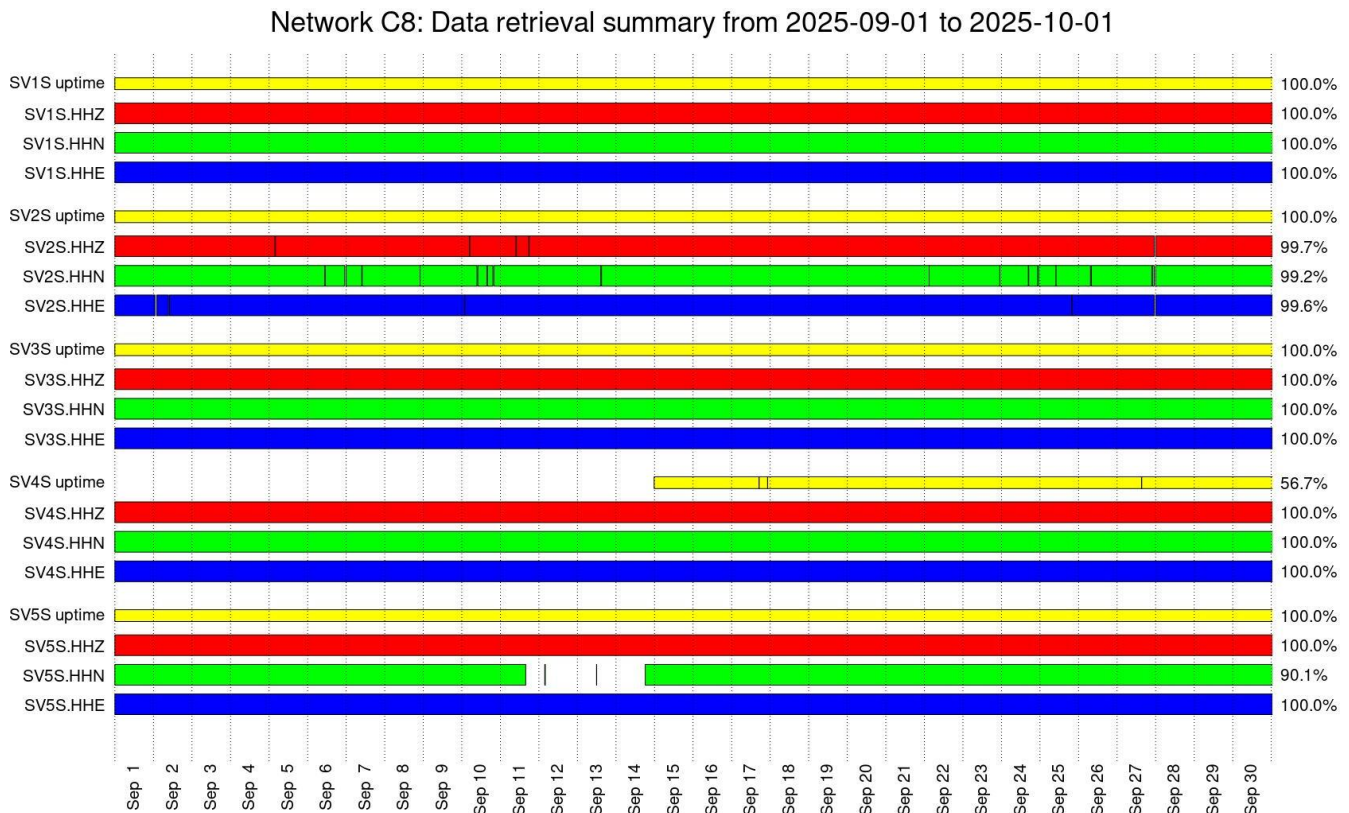


Figure 1. Retrieved data intervals for all channels (red, green, and blue bars) and uptimes (yellow). Total percentages of measured uptime and data retrieval are shown on the right.

State of health for station C8.SV1S (NE01) from 2025-09-01 to 2025-10-01

Power supply voltage

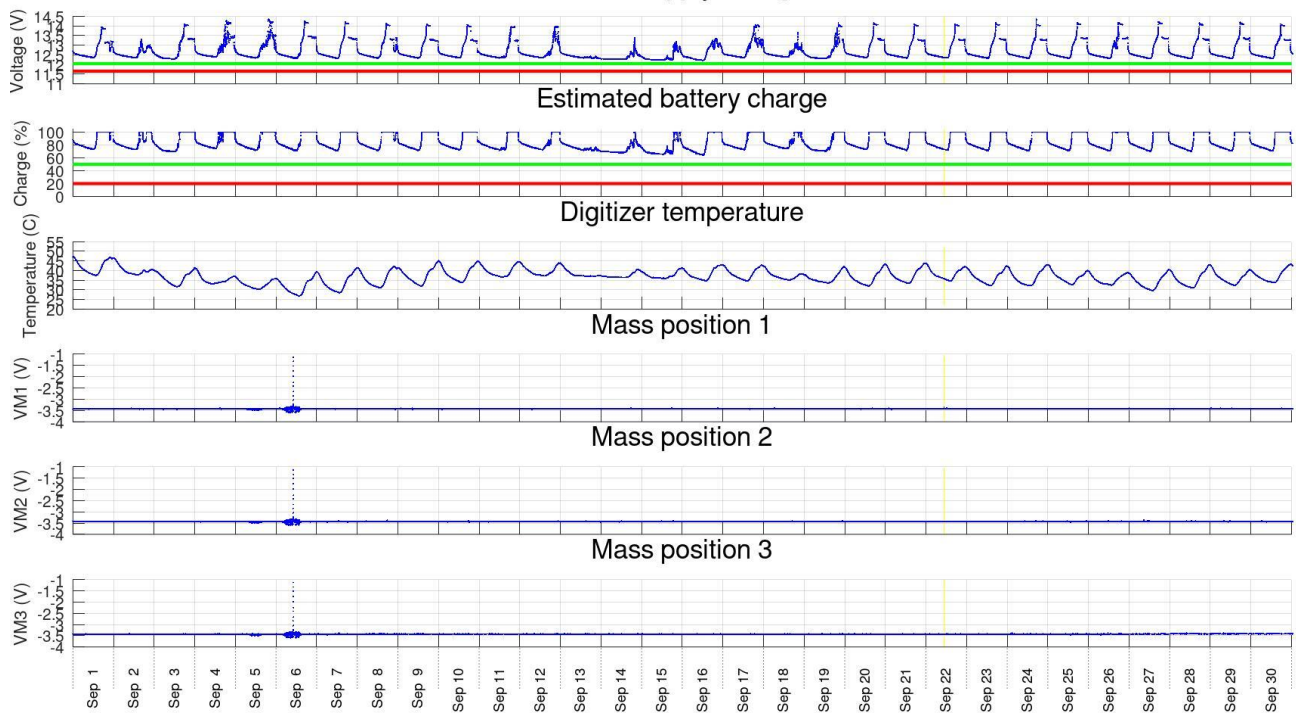


Figure 2. State of health parameters for each station (SV1S here). Image headings: power supply voltage, estimated battery charge levels, temperature on board, voltages measuring mass positions.

State of health for station C8.SV2S (SW01) from 2025-09-01 to 2025-10-01

Power supply voltage

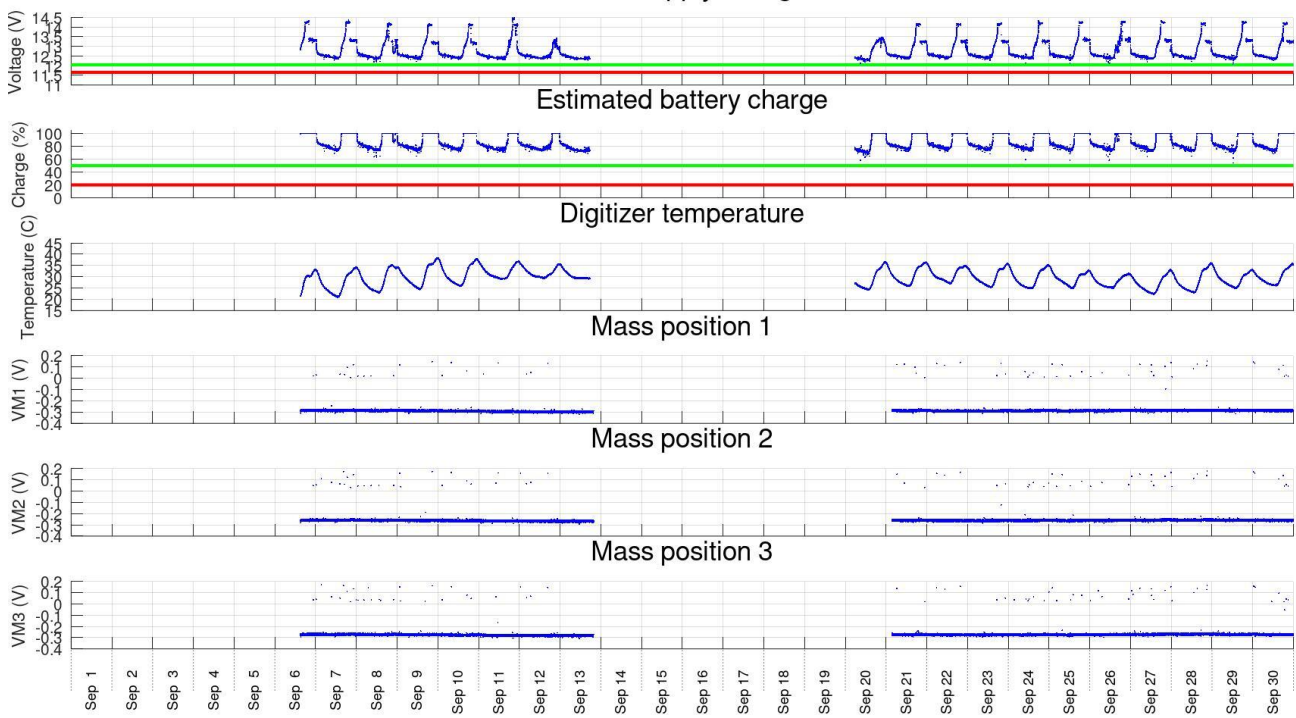


Figure 2, continued, station SV2S.

State of health for station C8.SV3S (NW01) from 2025-09-01 to 2025-10-01

Power supply voltage

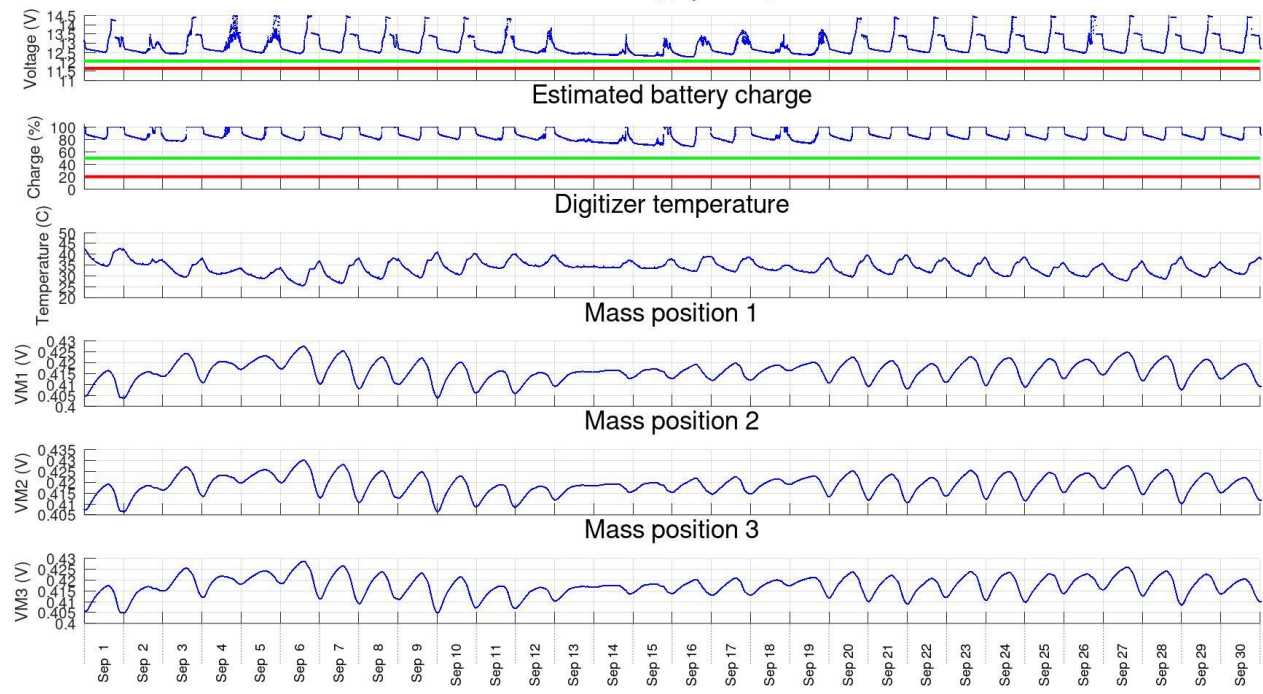


Figure 2, continued, station SV3S.

State of health for station C8.SV4S (SE01) from 2025-09-01 to 2025-10-01

Power supply voltage

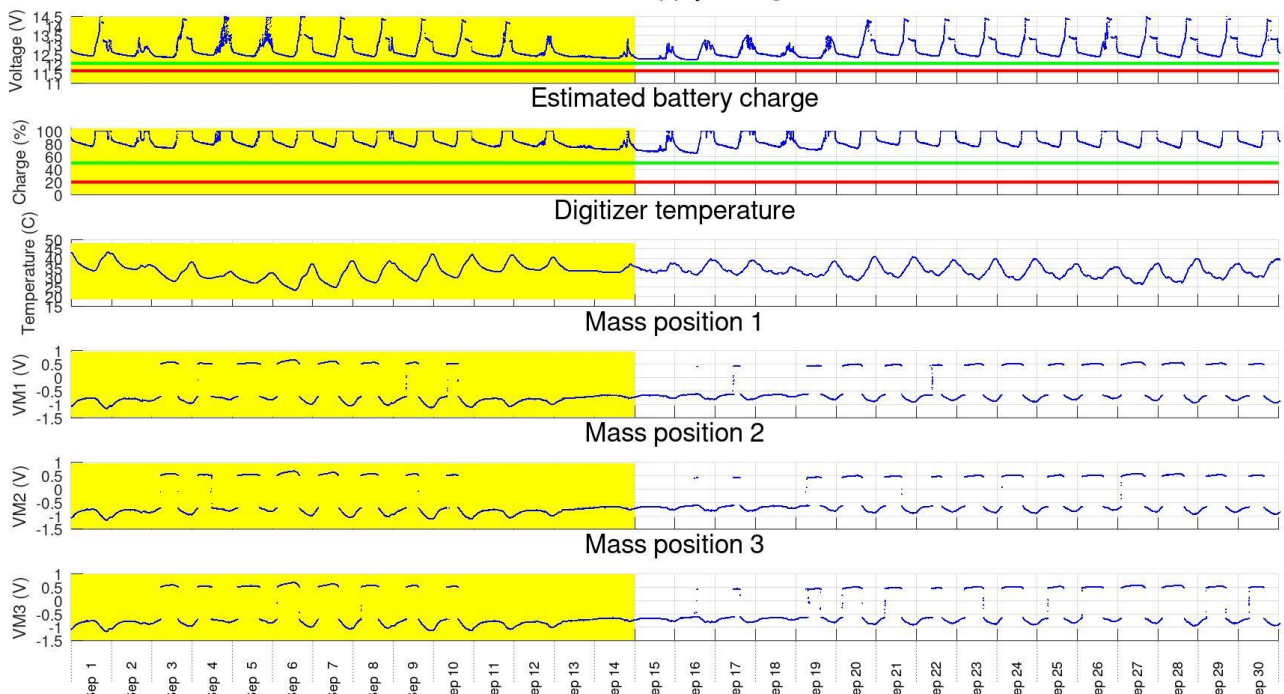


Figure 2, continued, station SV4S.

State of health for station C8.SV5S (NE02) from 2025-09-01 to 2025-10-01

Power supply voltage

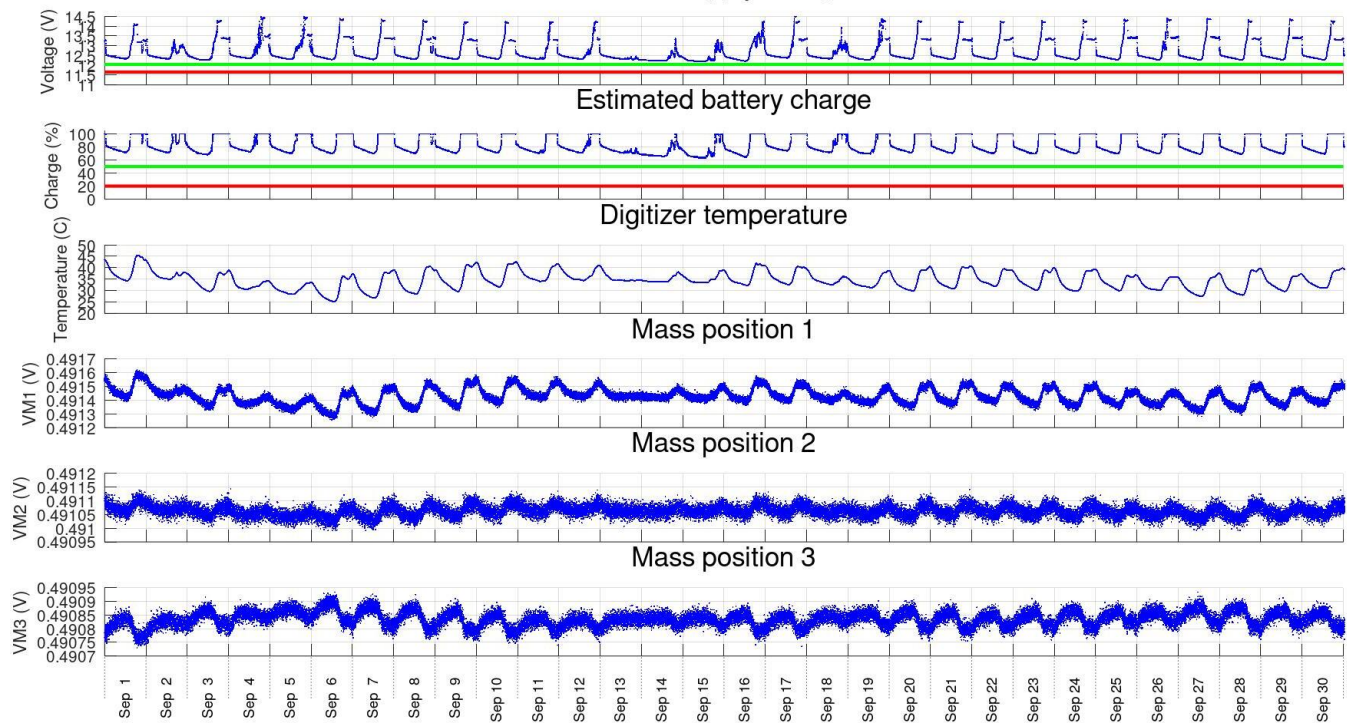


Figure 2, continued, station SV5S.

2. Data quality

Figure 3 shows two measures of data quality evaluated for each channel:

- 1) Numbers of spikes and tears (sharp changes of DC level) within 1-hour time intervals;
- 2) 1-hour root-mean square (RMS) average amplitudes in each channel.

From station SV2S, no data were received, and it is not shown in Figure 3 .

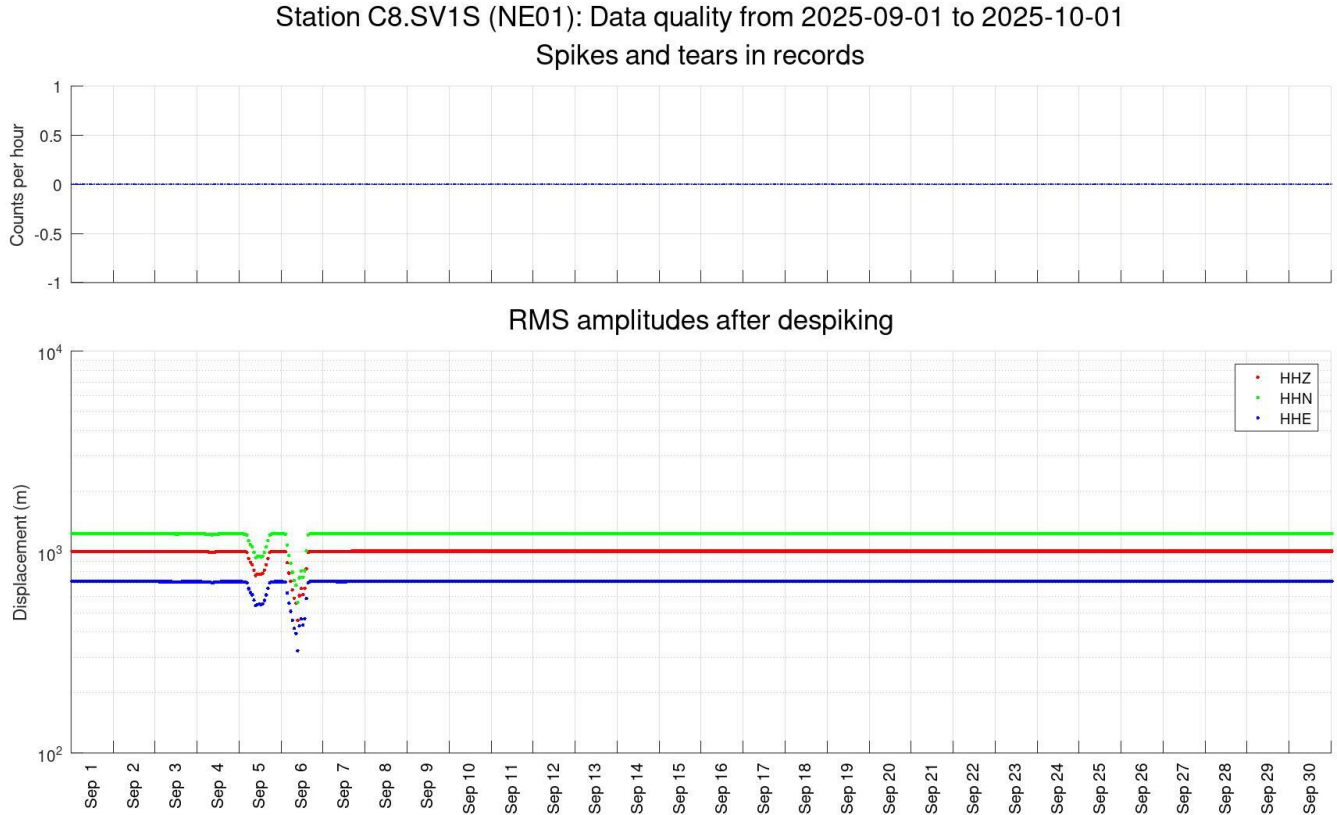


Figure 3. Measures of data quality in hour-long intervals. Station names and time intervals are indicated in plot headings (SV1S in this plot). Red, green, and blue colors correspond to channels HHZ, HHN, and HHE, respectively (as in Figure 1).

Top panels: Numbers of spikes and tears per hour auto-detected in data records.

Bottom panels: RMS ground displacements (meters).

Station C8.SV2S (SW01): Data quality from 2025-09-01 to 2025-10-01
 Spikes and tears in records

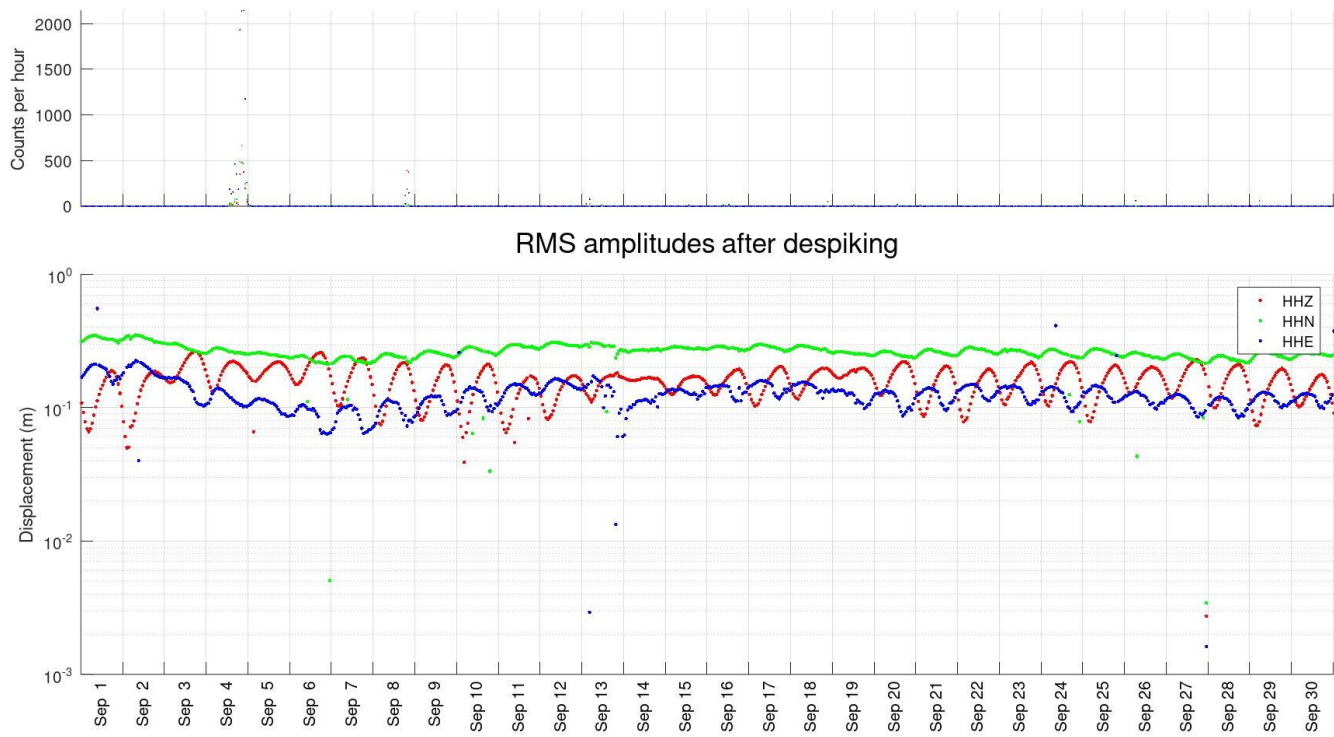


Figure 3, continued. Station SV2S.

Station C8.SV3S (NW01): Data quality from 2025-09-01 to 2025-10-01
 Spikes and tears in records

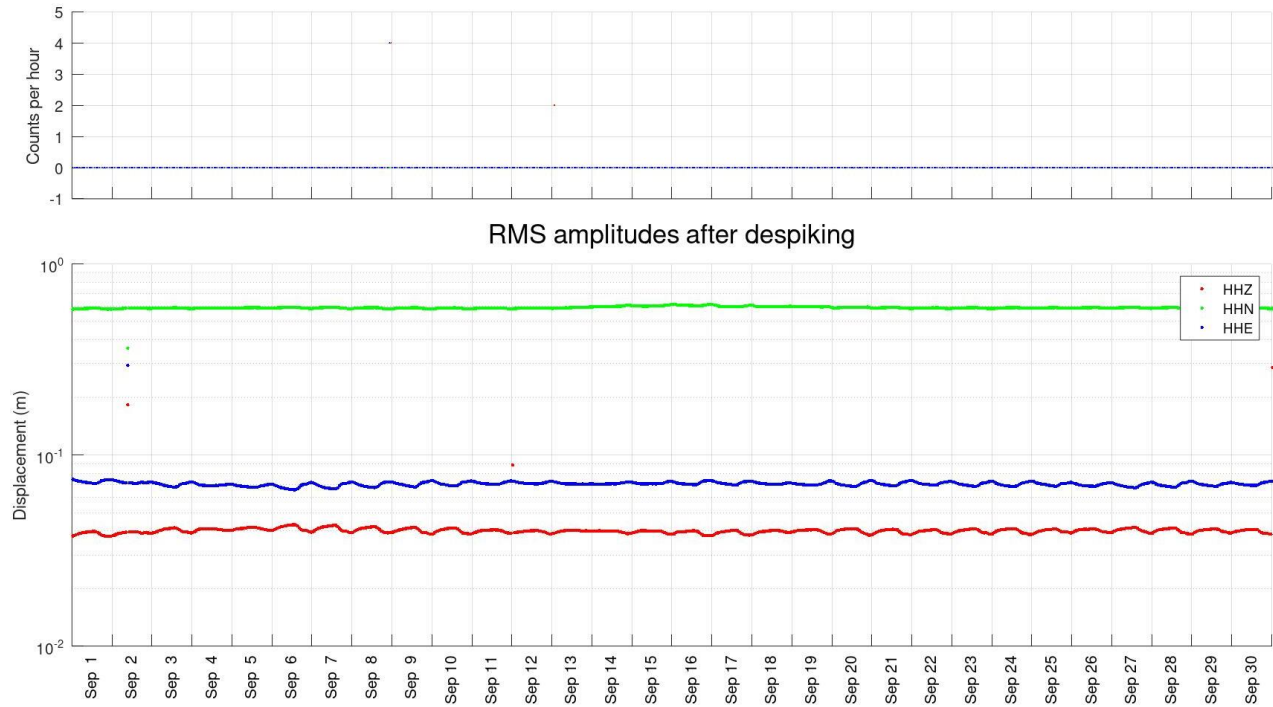


Figure 3, continued. Station SV3S. Sensor cable appears faulty in this station.

Station C8.SV4S (SE01): Data quality from 2025-09-01 to 2025-10-01

Spikes and tears in records

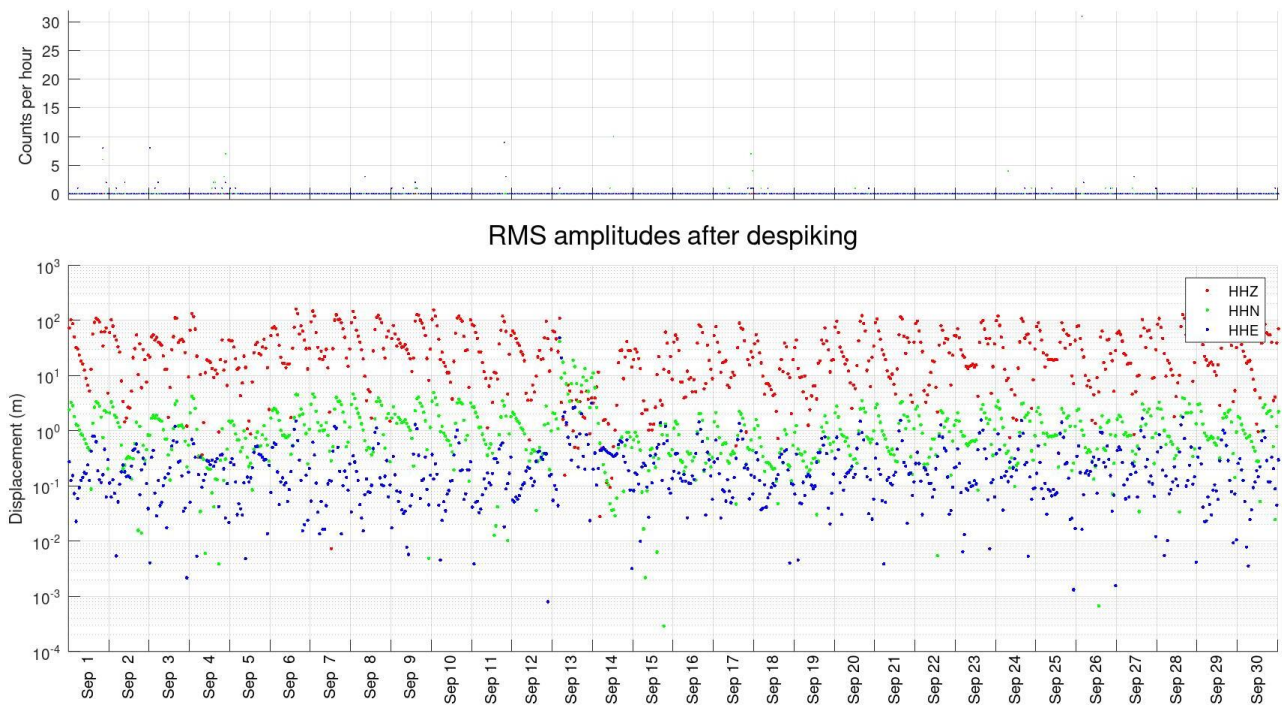


Figure 3, continued. Station SV4S.

Station C8.SV5S (NE02): Data quality from 2025-09-01 to 2025-10-01

Spikes and tears in records

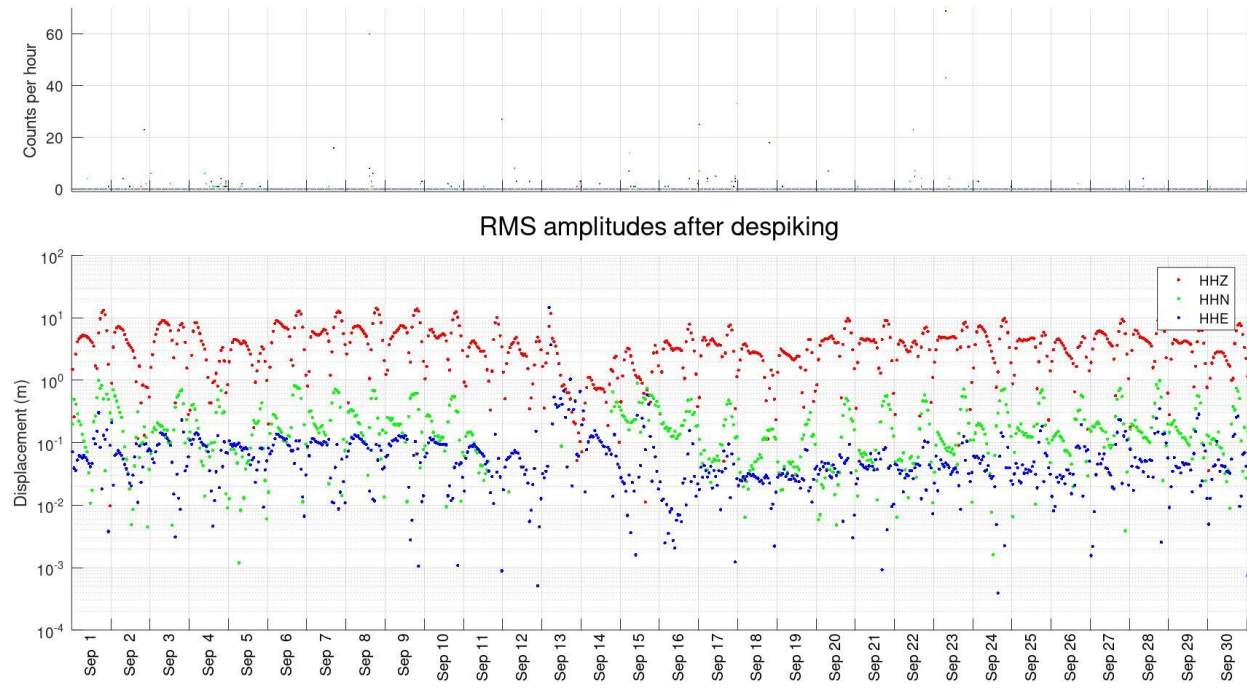


Figure 3, continued. Station SV5S

3. Processing procedure and parameters

The data processing procedure was described in previous reports. Parameters of the STA/LTA algorithm in two frequency bands are shown in Table 1. Only one frequency band (#1) is currently used.

Table 1. STA/LTA algorithm parameters

Parameter	For regional events	For local and target events
Filter band 1	0.5 – 10 Hz	3 – 20 Hz
Filter band 2	3 – 50 Hz	10 – 50 Hz
STA window	3 s	0.2 s
LTA window	15 s	2 s
Floor on normalized STA/LTA ratio	0.5	0.6
Maximum accepted STA/LTA ratio	0.99	0.99
Relative level of triggering	0.5	0.5
Relative level of detriggering	0.5	0.5
Number of channels for triggering	3	3

4. Seismic event detection

The classification of seismic events used in these reports and numbers of events detected in September 2025 are shown in Table 2.

Table 2. Classification of seismic events detected at Aquistore broadband seismic array

Event class code	Class name	Identification criteria	Number of detections in this report
1	Teleseismic	Hypocentral distance $D > 1000$ km, presence in catalogues	26
2	Regional	$100 < D < 1000$ km, presence in catalogues	0
3	Local	Approx. $4 < D < 100$ km	-----
3a	Possible mine blasts	Characteristic waveforms, amplitudes, back-azimuths east of Aquistore, D about 12-15 km	17

3b	Mining-related	Low frequencies, extended repeated wavetrains low arrival velocities related to surface waves	2 (selected from numerous occurrences)
4	Proximity (close local)	$D < 3-4$ km, deviation of array moveouts from plane-wave patterns, high frequency	-----
4a*	Surface sources near array	Large travel-time moveouts, variable back-azimuths	3*
4b*	Target zone	Source at recognizable nonzero depth, small travel-time moveouts, high frequency	0*

*) Because of using only three stations, classes 4a and 4b are not differentiated in current report.

Automatic detections

The procedure of multichannel automatic detections is currently being revised and not shown in the present report.

Event bulletins

Earthquake data bulletins for the period of this report were obtained from NEIC (USGS) and NRCan web services (Figure). Events larger than magnitude 2.5 were taken from USGS, and all available events obtained from NRCan. Events with magnitudes above the selected $magnitude \propto distance^{1.5}$ threshold (dashed green line in Figure) were reviewed interactively (next section).

Events from 2025-09-01 to 2025-10-01

25 regional

1732 teleseismic

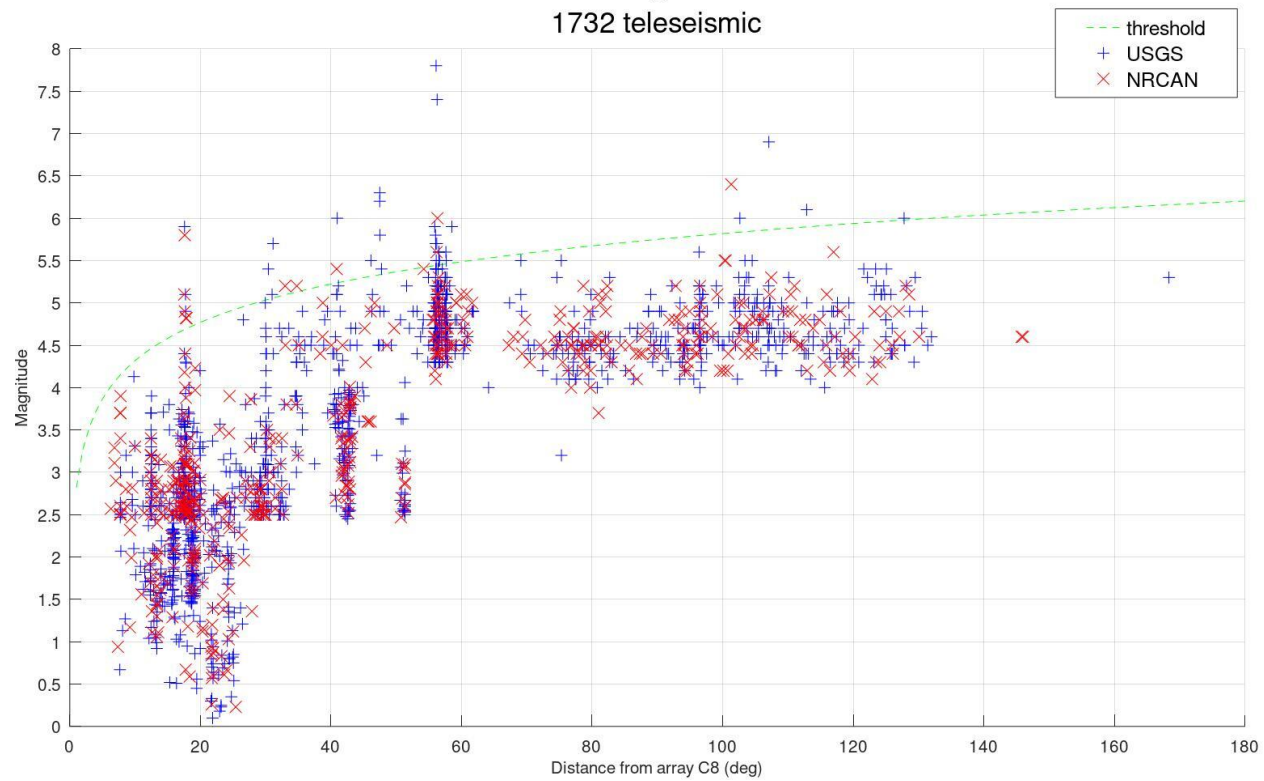


Figure 5. Magnitudes and distances from Aquistore for earthquake parameters downloaded from USGS and NRCAN databases (legend). Dashed green line shows the detection threshold above which a manual review of events was performed.

Teleseismic events (class 1)

Above the threshold line in Figure 5, 26 teleseismic events (class 1 in Table 2) were identified in September 2025 (Figure 6).

Time zeros in Figure 6 plots are located at the times of P-wave arrivals at the Aquistore array predicted in the reference model IASP91, and blue bars near *time* = 0 are interactive picks of P-wave arrival times.

Note that only the correctly operating stations SV1S, SV4S, and SV5S are used in these and other data plots below.

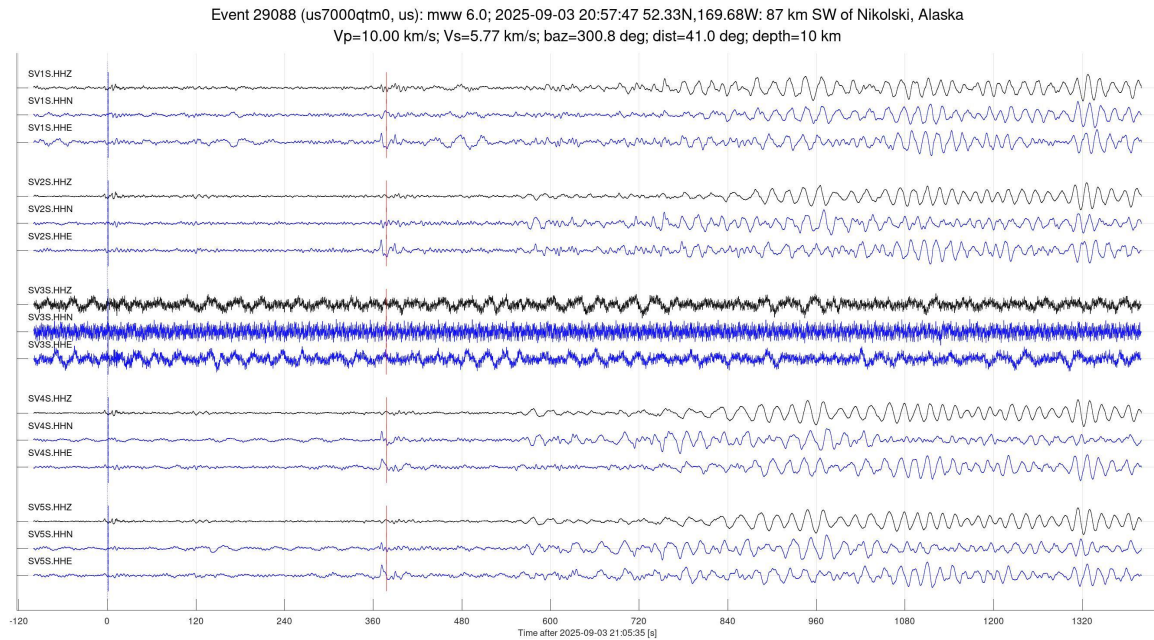


Figure 6. Sample teleseismic events detected at Aquistore in September 2025. Catalogue IDs, times, distances in degrees, source coordinates and localities, back-azimuths ('baz='), distances ('dist=') and source depths are shown in plot headings. Vertical-component records are shown in black, and horizontal components in blue. Colour bars above some records show single-channel STA/LTA values for accepted detections of these events.

Event 29574 (20250907.1500001, cn): -- 4.8; 2025-09-07 15:00:08 51.33N,130.66W: 231 km WNW of Port Hardy BC
 $V_p=10.00$ km/s; $V_s=5.77$ km/s; $\text{baz}=287.7$ deg; $\text{dist}=17.8$ deg; $\text{depth}=10$ km

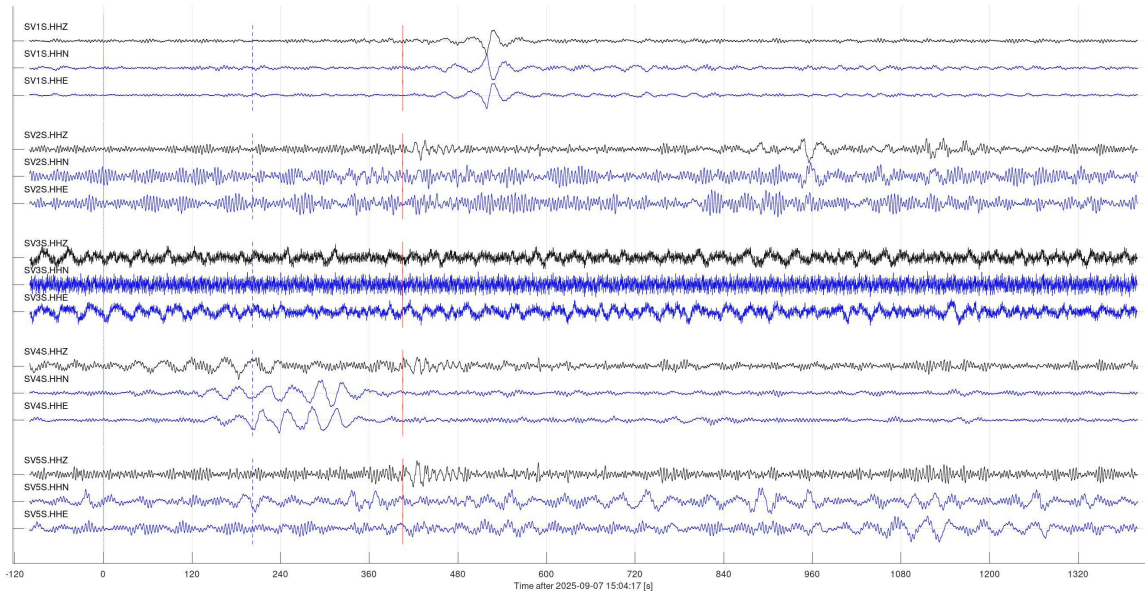


Figure 6, continued.

Event 29582 (us7000quxl, us): mb 4.9; 2025-09-09 05:59:03 42.43N,126.49W: 167 km WSW of Port Orford, Oregon
 $V_p=10.00$ km/s; $V_s=5.77$ km/s; $\text{baz}=256.6$ deg; $\text{dist}=17.6$ deg; $\text{depth}=11$ km

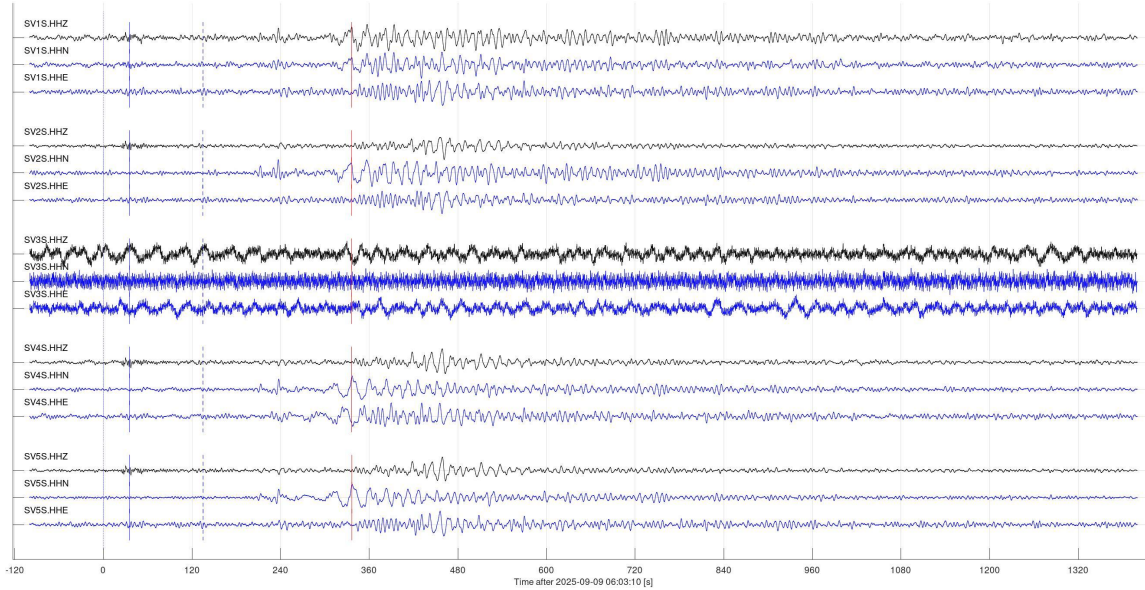


Figure 6, continued.

Event 29588 (us7000quwy, us): mww 5.8; 2025-09-09 04:08:01 42.37N,126.44W: 165 km WSW of Port Orford, Oregon
 $V_p=10.00$ km/s; $V_s=5.77$ km/s; $\text{baz}=256.4$ deg; $\text{dist}=17.6$ deg; $\text{depth}=14$ km

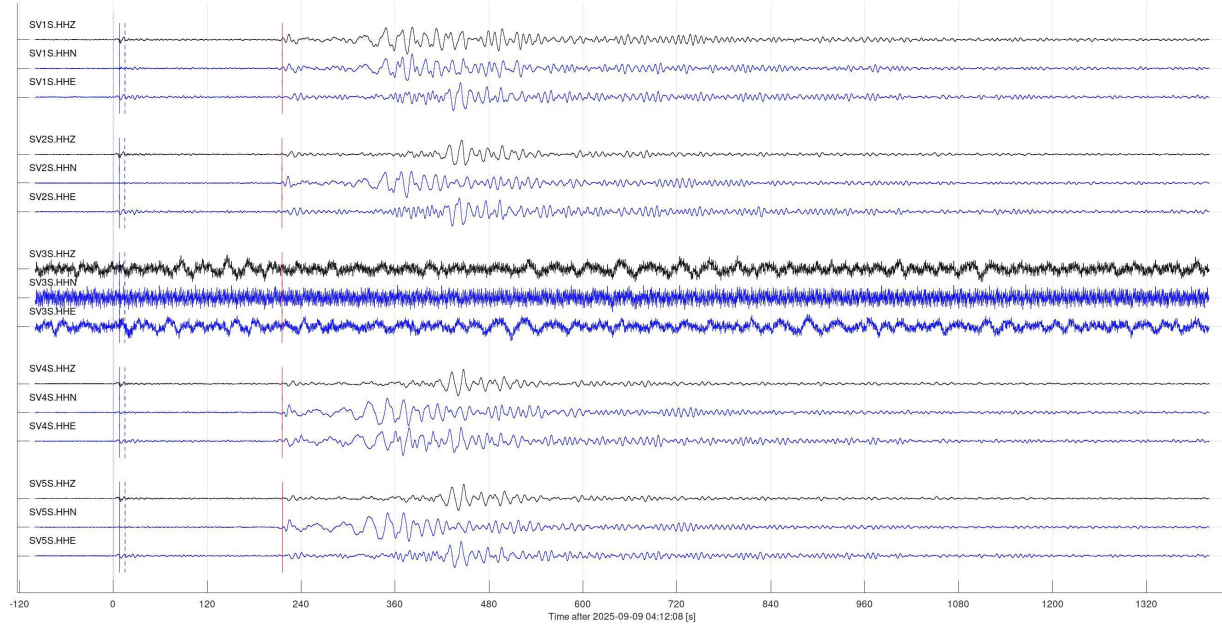


Figure 6, continued.

Event 29617 (20250907.1500003, cn): -- 4.8; 2025-09-07 15:00:07 51.24N,130.85W: 241 km WNW of Port Hardy BC
 $V_p=10.00$ km/s; $V_s=5.77$ km/s; $\text{baz}=287.5$ deg; $\text{dist}=17.9$ deg; $\text{depth}=10$ km

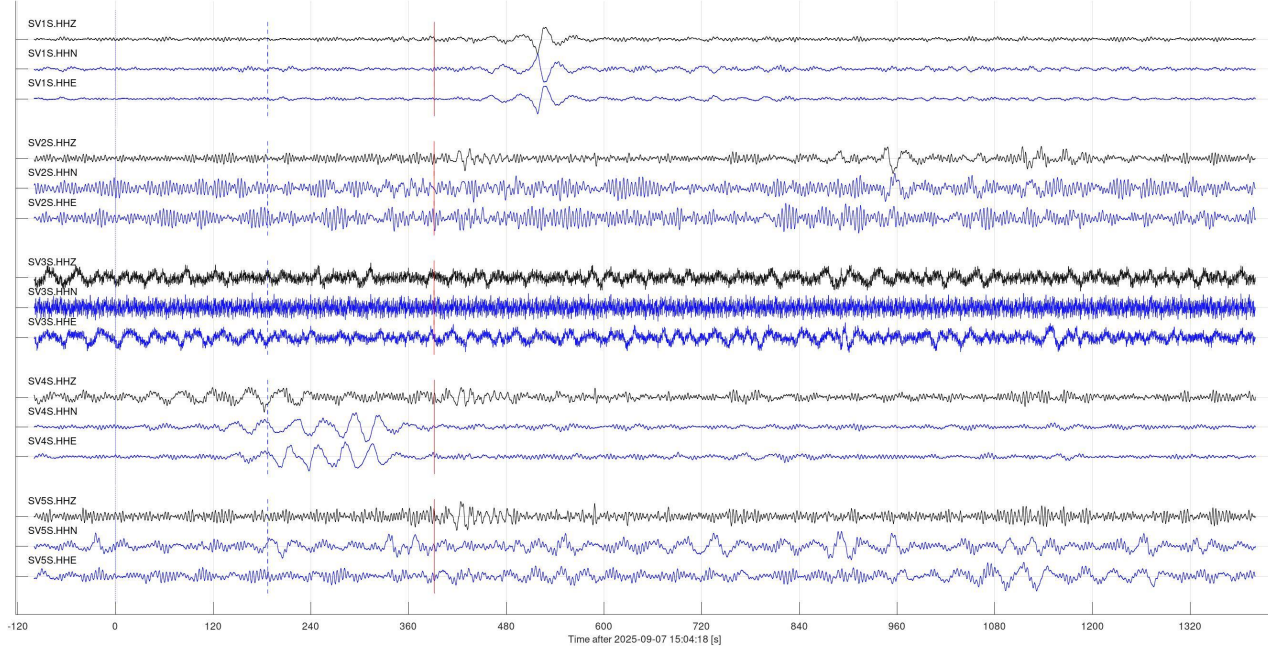


Figure 6, continued.

Event 29675 (us7000qv3g, us): mww 5.1; 2025-09-09 19:31:44 42.44N,126.67W: 181 km WSW of Port Orford, Oregon
 Vp=10.00 km/s; Vs=5.77 km/s; baz=256.8 deg; dist=17.7 deg; depth=10 km

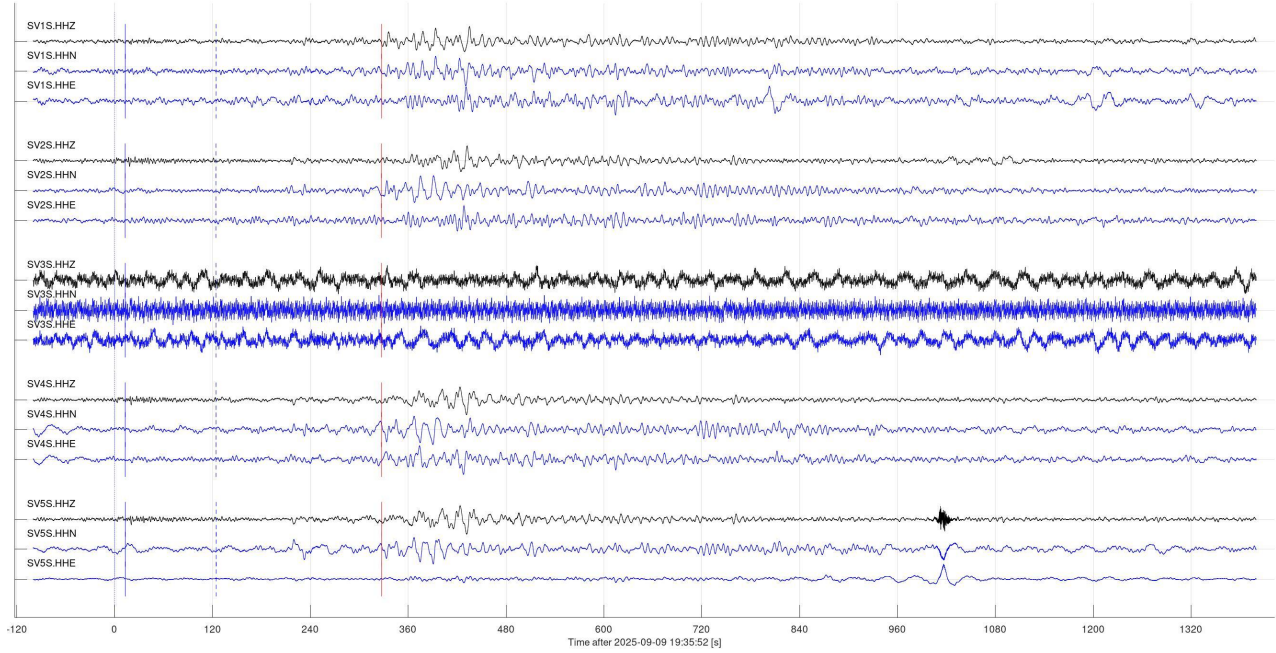


Figure 6, continued.

Event 29678 (us7000qv38, us): mww 4.9; 2025-09-09 19:02:04 42.38N,126.65W: 181 km WSW of Port Orford, Oregon
 Vp=10.00 km/s; Vs=5.77 km/s; baz=256.6 deg; dist=17.7 deg; depth=10 km

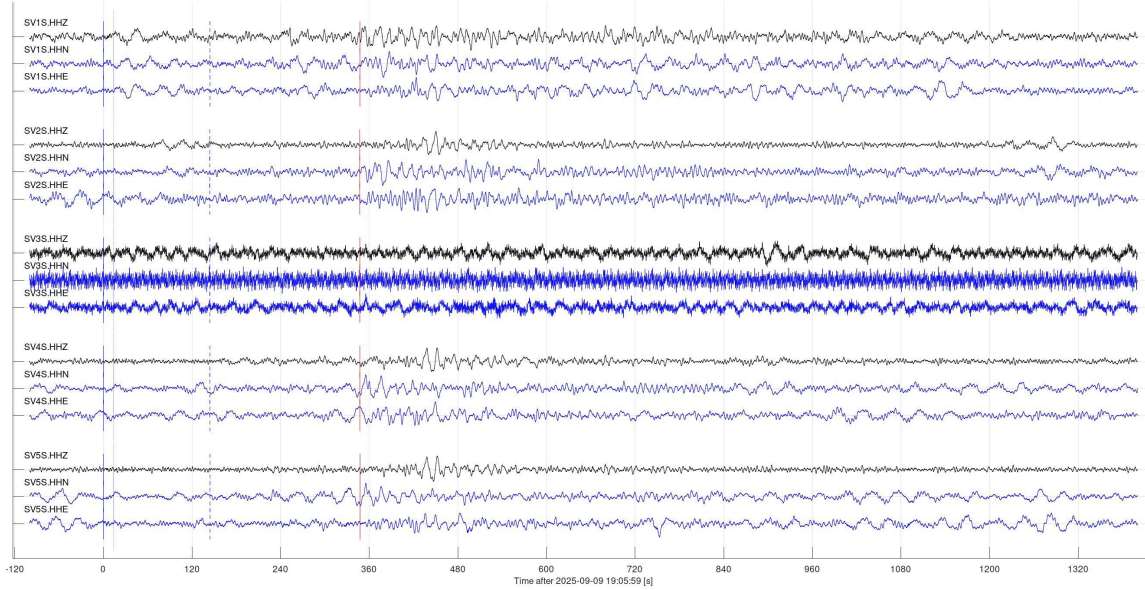


Figure 6, continued.

Event 29875 (us7000qvw5, us): mww 7.4; 2025-09-13 02:37:55 53.10N,160.29E: 111 km E of Petropavlovsk-Kamchatsky, Russia
 Vp=10.00 km/s; Vs=5.77 km/s; baz=313.9 deg; dist=56.3 deg; depth=39 km

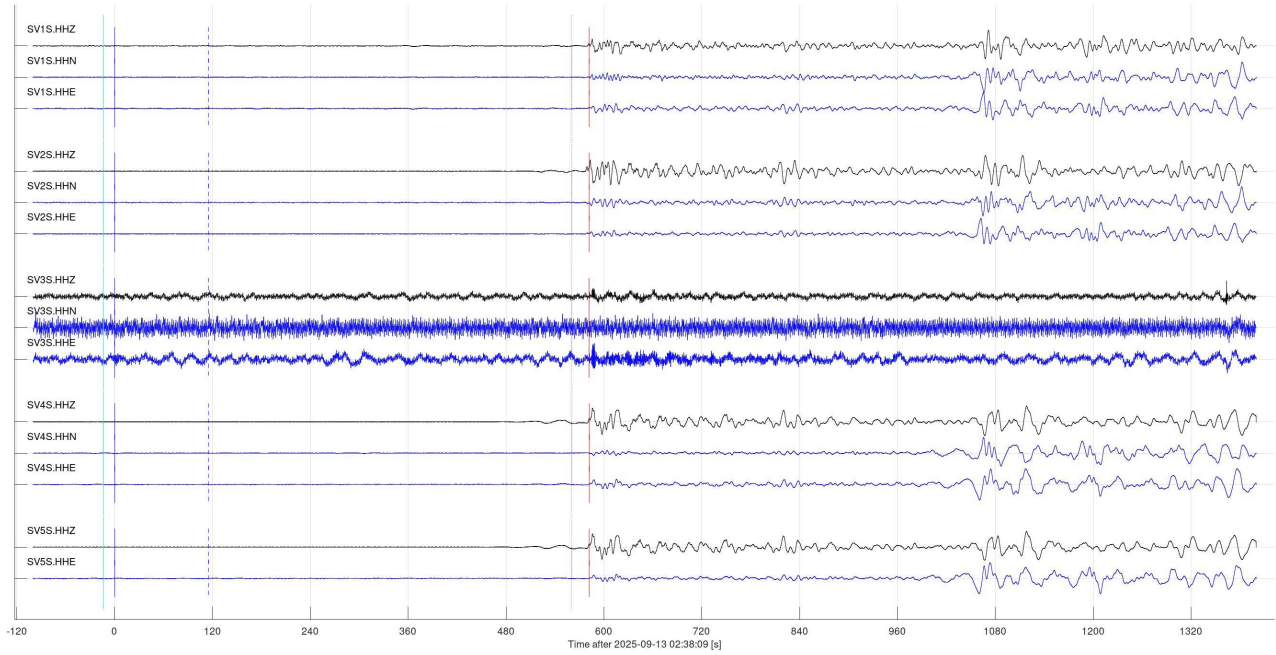


Figure 6, continued.

Event 30033 (us7000qwch, us): mww 6.0; 2025-09-15 16:34:37 52.69N,160.70E: 145 km ESE of Petropavlovsk-Kamchatsky, Russia
 Vp=10.00 km/s; Vs=5.77 km/s; baz=313.4 deg; dist=56.3 deg; depth=24 km

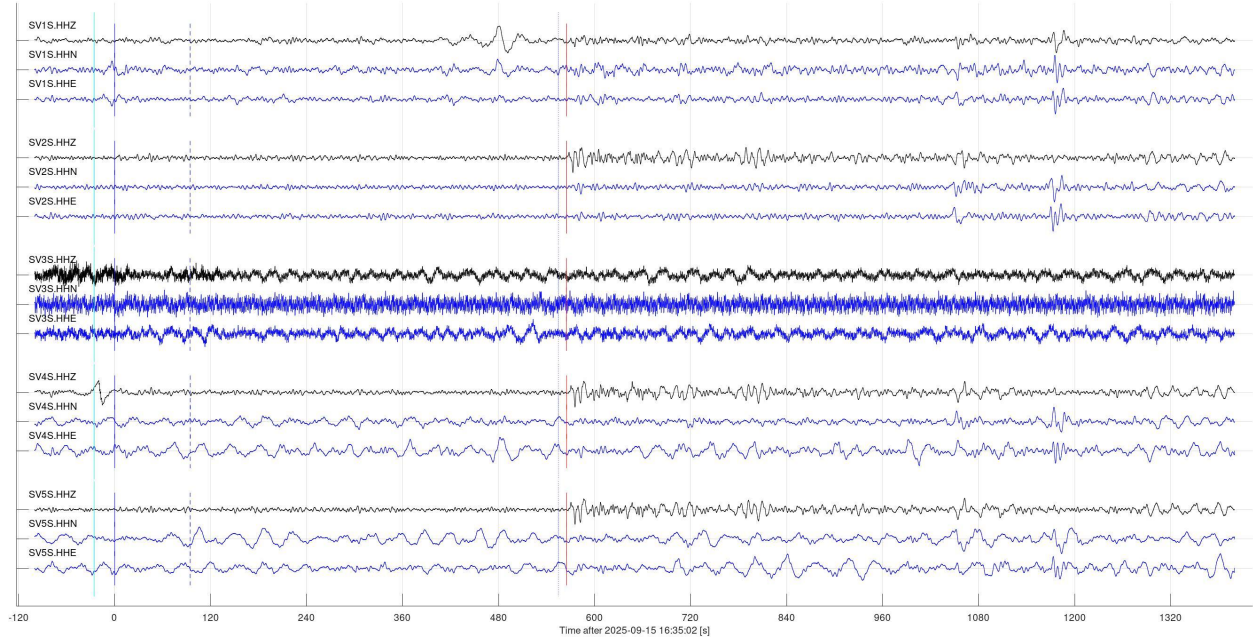


Figure 6, continued.

Event 30218 (us7000qx2q, us): mb 5.8; 2025-09-18 19:08:20 52.97N,160.96E: 157 km E of Petropavlovsk-Kamchatsky, Russia
 $V_p=10.00$ km/s; $V_s=5.77$ km/s; $\text{baz}=313.5$ deg; $\text{dist}=56.0$ deg; depth=10 km

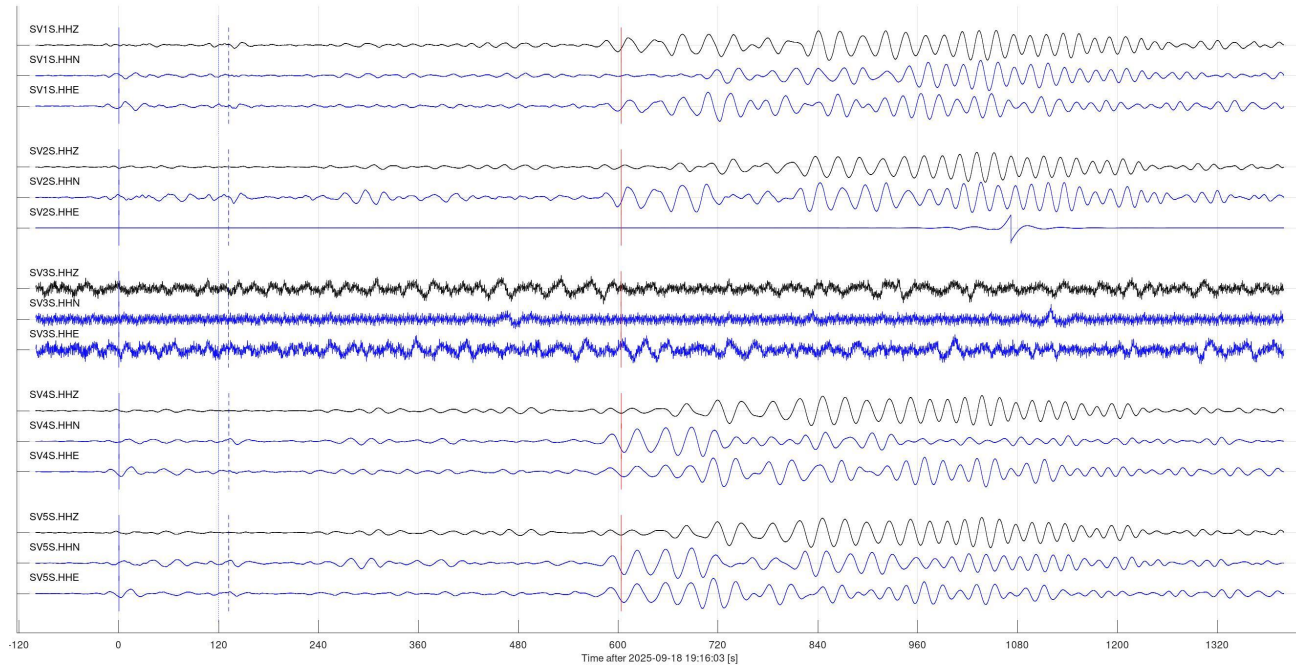


Figure 6, continued.

Event 30221 (us7000qx2g, us): mww 7.8; 2025-09-18 18:58:14 53.19N,160.51E: 127 km E of Petropavlovsk-Kamchatsky, Russia
 $V_p=10.00$ km/s; $V_s=5.77$ km/s; $\text{baz}=313.9$ deg; $\text{dist}=56.1$ deg; depth=20 km

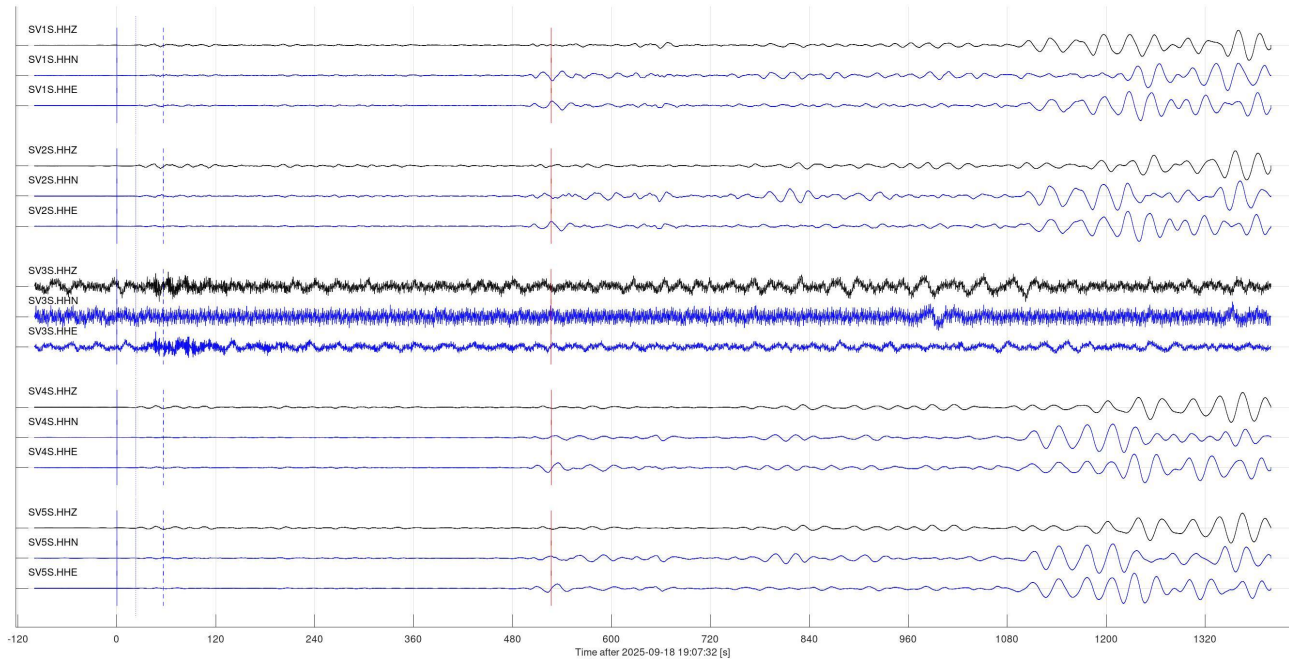


Figure 6, continued.

Event 30284 (us7000qxcr, us): mww 5.9; 2025-09-19 15:45:35 52.94N,161.28E: 178 km E of Petropavlovsk-Kamchatsky, Russia
 $V_p=10.00$ km/s; $V_s=5.77$ km/s; $\text{baz}=313.3$ deg; $\text{dist}=55.9$ deg; $\text{depth}=10$ km

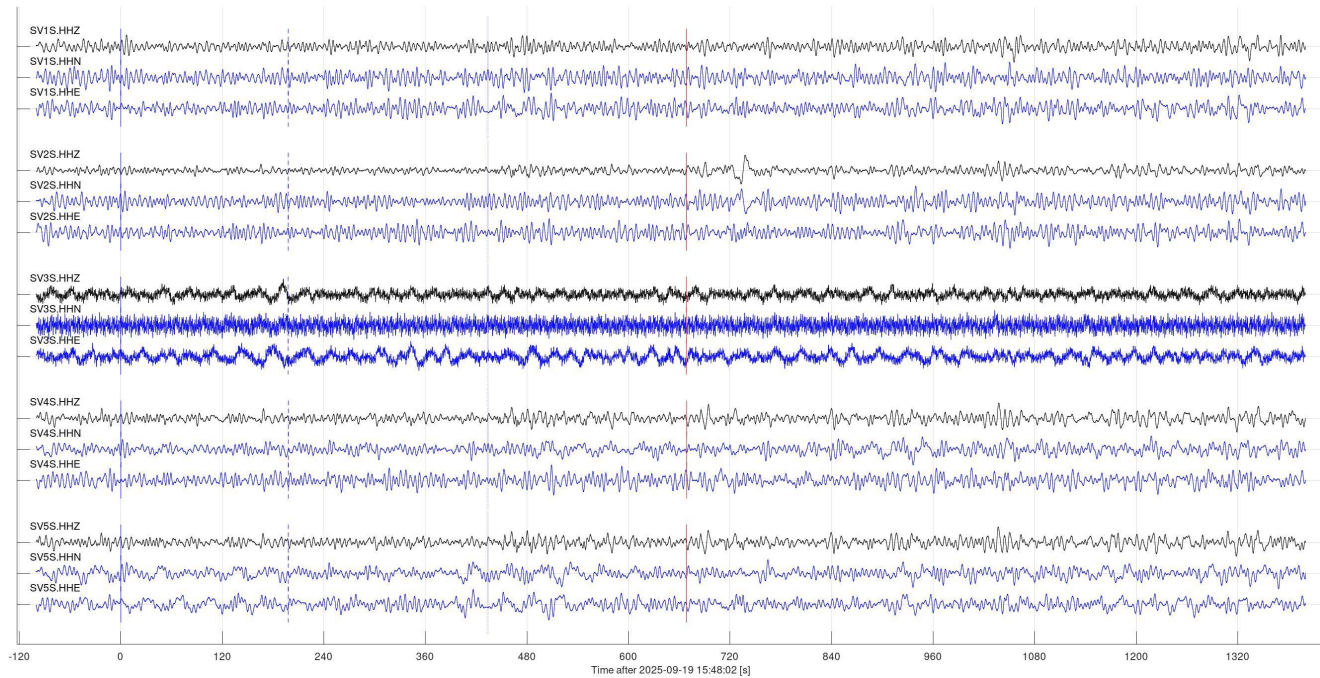


Figure 6, continued.

Event 30287 (us7000qxcd, us): mww 5.9; 2025-09-19 14:55:29 51.42N,157.79E: 90 km E of Ozernovskiy, Russia
 $V_p=10.00$ km/s; $V_s=5.77$ km/s; $\text{baz}=313.5$ deg; $\text{dist}=58.5$ deg; $\text{depth}=84$ km

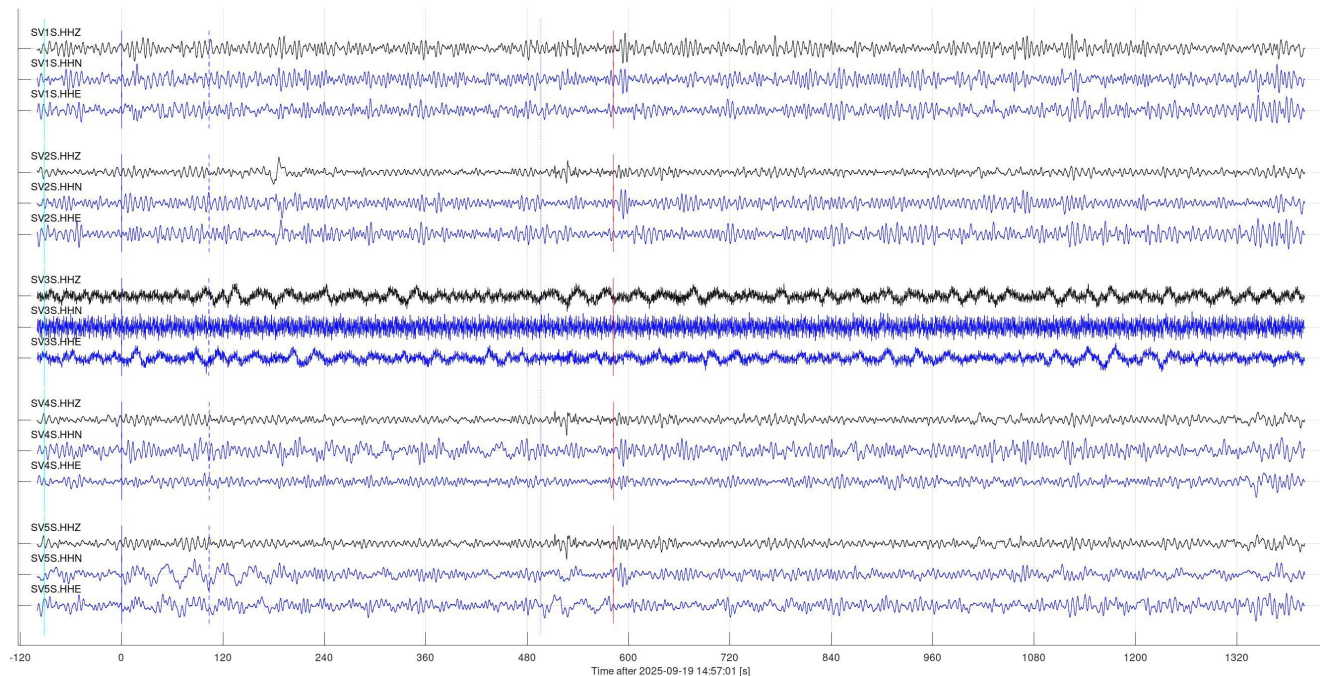


Figure 6, continued.

Event 30290 (us7000qxat, us): mww 5.5; 2025-09-19 13:27:04 52.24N,160.65E: 164 km SE of Petropavlovsk-Kamchatsky, Russia
 Vp=10.00 km/s; Vs=5.77 km/s; baz=313.0 deg; dist=56.6 deg; depth=10 km

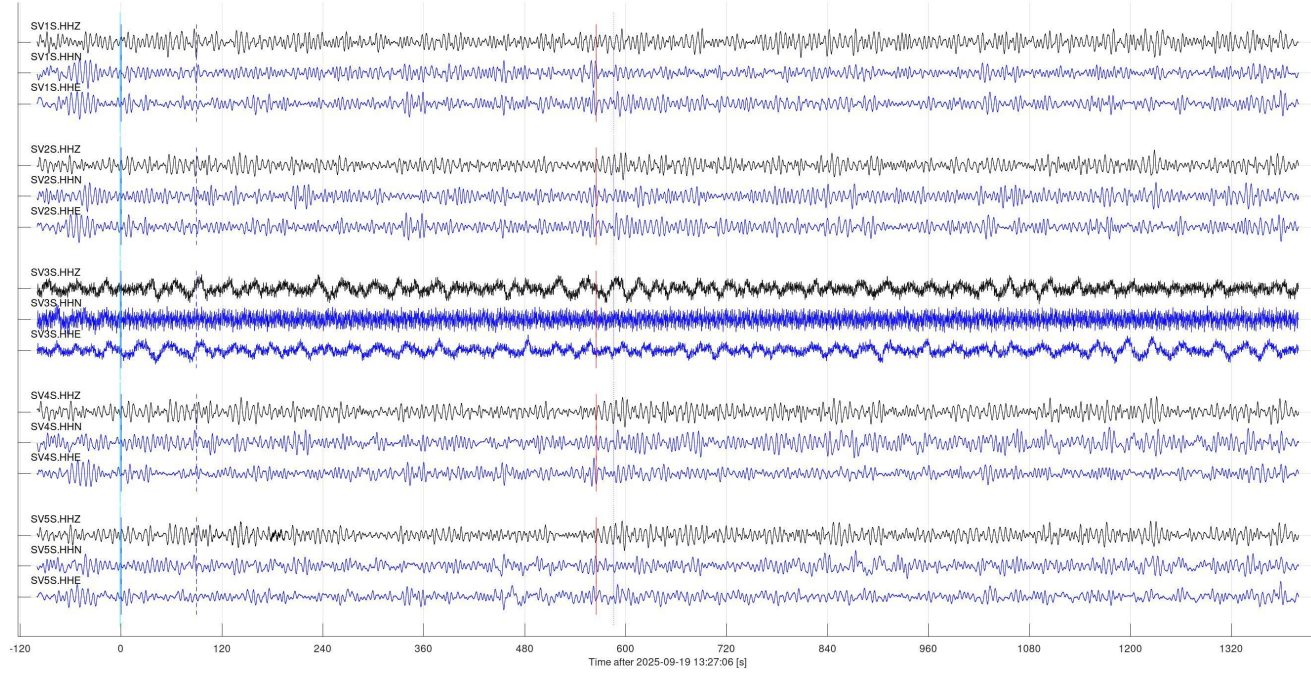


Figure 6, continued.

Event 30504 (us6000rc4t, us): mww 5.6; 2025-09-22 18:18:54 51.43N,159.68E: 188 km SSE of Vilyuchinsk, Russia
 Vp=10.00 km/s; Vs=5.77 km/s; baz=312.6 deg; dist=57.6 deg; depth=17 km

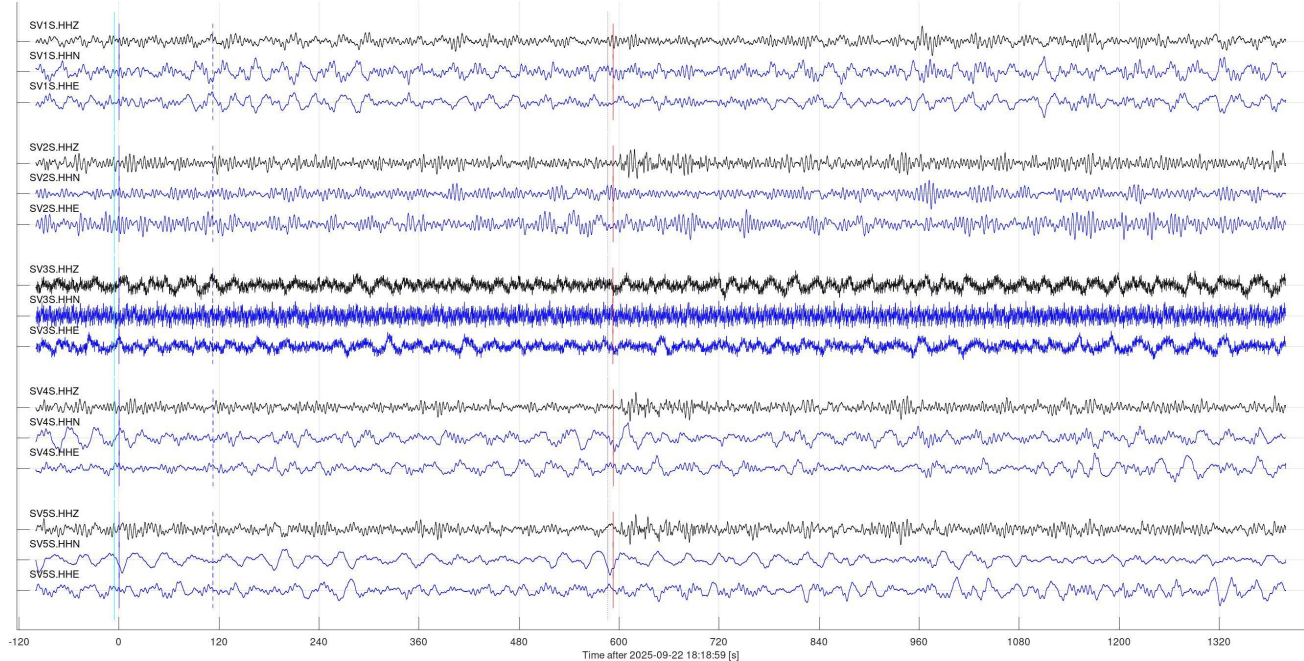


Figure 6, continued.

Event 30508 (us6000rc2r, us): mww 5.5; 2025-09-22 16:28:53 51.43N,159.54E: 184 km SSE of Vilyuchinsk, Russia
 $V_p=10.00$ km/s; $V_s=5.77$ km/s; $\text{baz}=312.7$ deg; $\text{dist}=57.7$ deg; $\text{depth}=10$ km

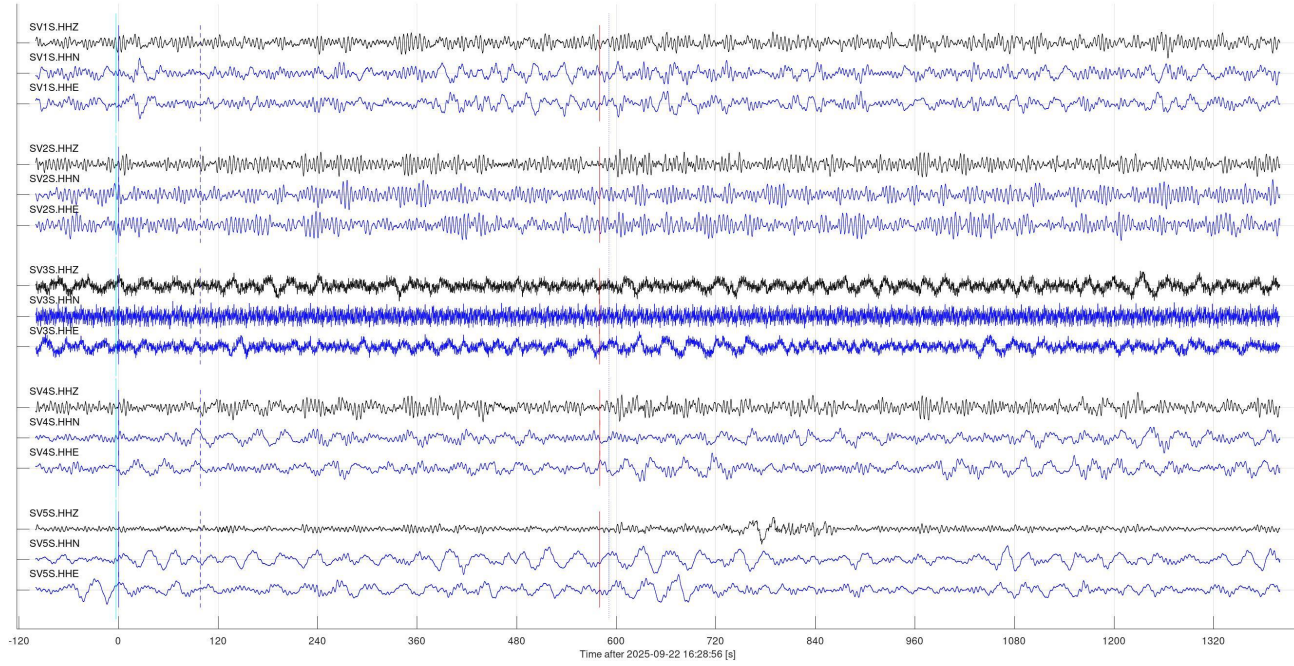


Figure 6, continued.

Event 30512 (us7000qxtz, us): mww 5.4; 2025-09-22 14:24:10 18.73N,106.33W: 159 km SW of José María Morelos, Mexico
 $V_p=10.00$ km/s; $V_s=5.77$ km/s; $\text{baz}=186.1$ deg; $\text{dist}=30.4$ deg; $\text{depth}=10$ km

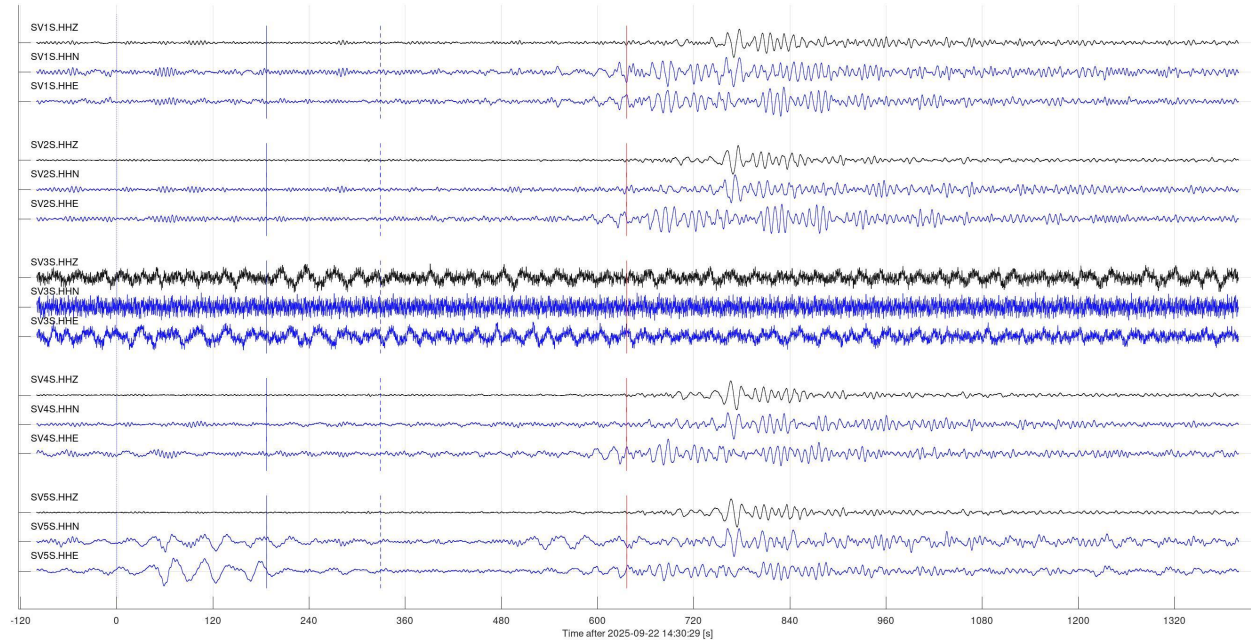


Figure 6, continued.

Event 30604 (us6000rcqw, us): mww 6.3; 2025-09-25 03:51:40 9.93N,70.69W: 27 km ENE of Mene Grande, Venezuela
 Vp=10.00 km/s; Vs=5.77 km/s; baz=134.3 deg; dist=47.5 deg; depth=14 km

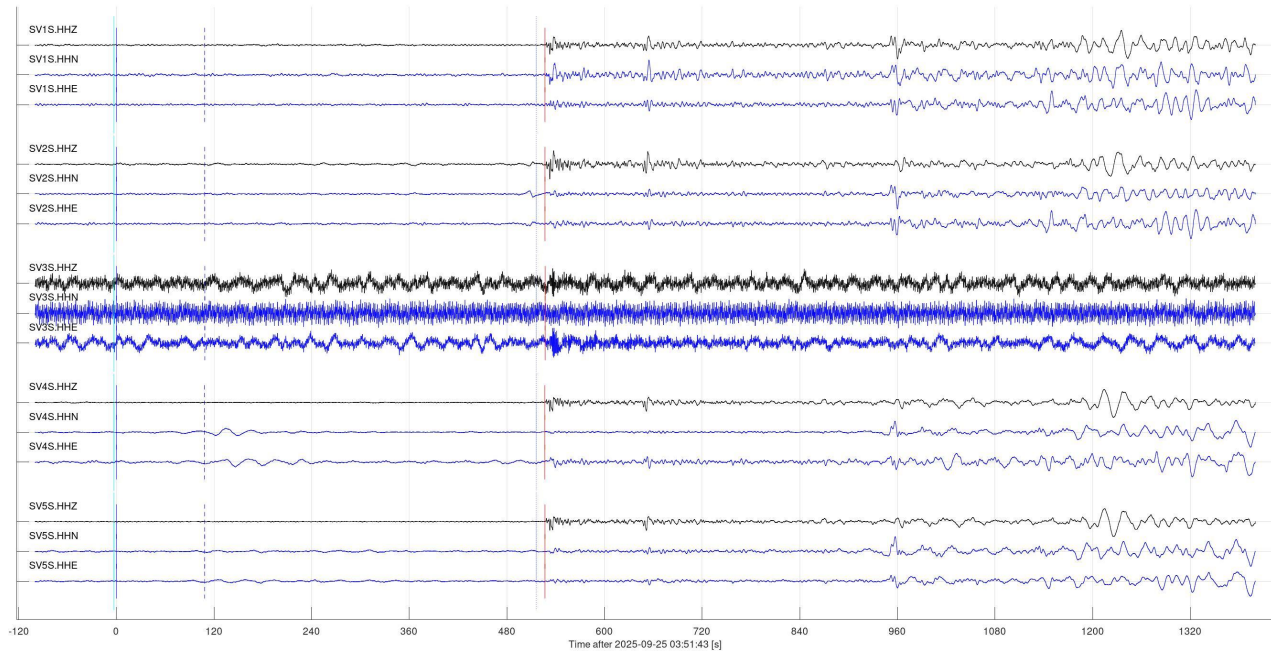


Figure 6, continued.

Event 30609 (us6000rcnw, us): mww 6.2; 2025-09-24 22:21:55 9.92N,70.72W: 24 km ENE of Mene Grande, Venezuela
 Vp=10.00 km/s; Vs=5.77 km/s; baz=134.3 deg; dist=47.5 deg; depth=7.82 km

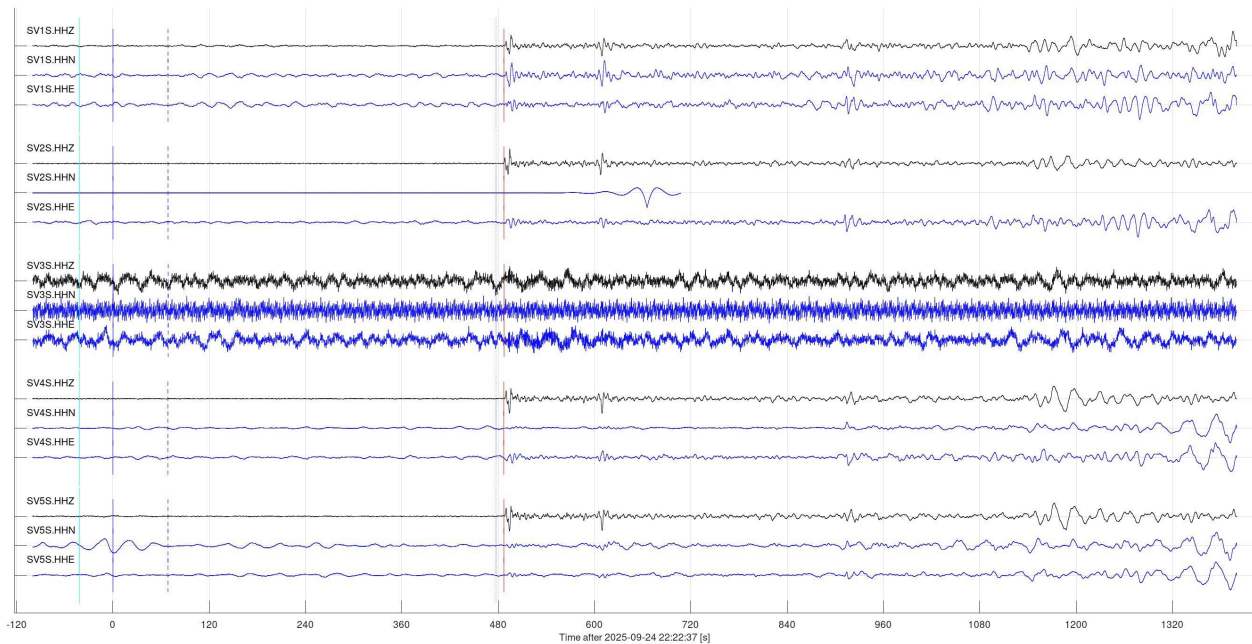


Figure 6, continued.

Event 30659 (us6000rd1w, us): mww 5.9; 2025-09-26 06:45:29 43.48N,127.22W: 231 km W of Bandon, Oregon
 Vp=10.00 km/s; Vs=5.77 km/s; baz=260.5 deg; dist=17.6 deg; depth=10 km

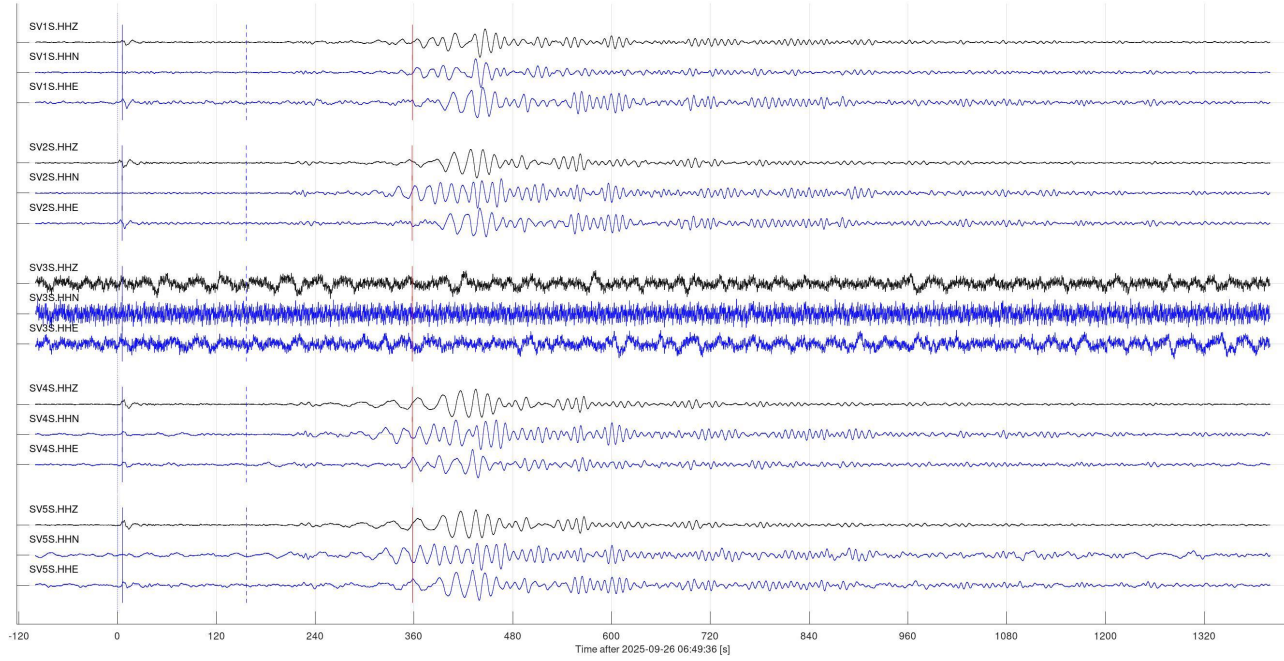


Figure 6, continued.

Event 30700 (us6000rcse, us): mb 5.1; 2025-09-25 10:21:21 18.12N,105.76W: 163 km SSW of Emiliano Zapata, Mexico
 Vp=10.00 km/s; Vs=5.77 km/s; baz=185.0 deg; dist=31.0 deg; depth=10 km

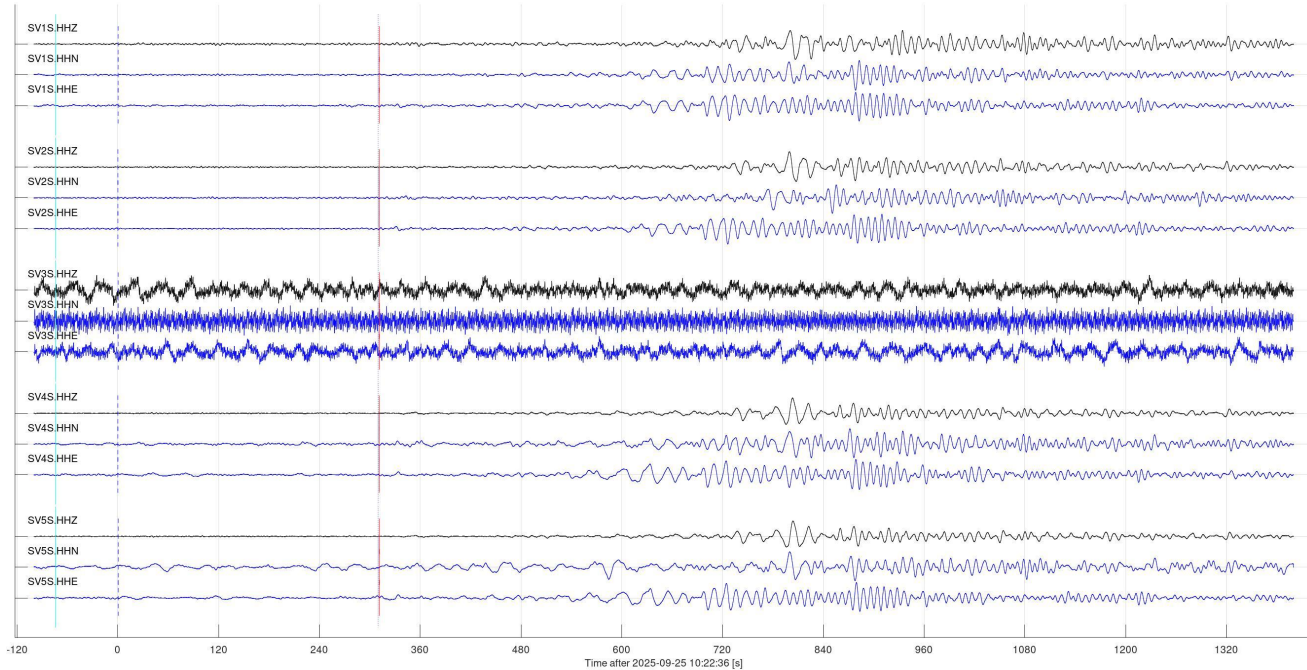


Figure 6, continued.

Event 30701 (us6000rcsb, us): mww 5.7; 2025-09-25 10:16:26 17.96N, 105.80W: 180 km SSW of Emiliano Zapata, Mexico
 $V_p=10.00$ km/s; $V_s=5.77$ km/s; $\text{baz}=185.0$ deg; $\text{dist}=31.1$ deg; $\text{depth}=10$ km

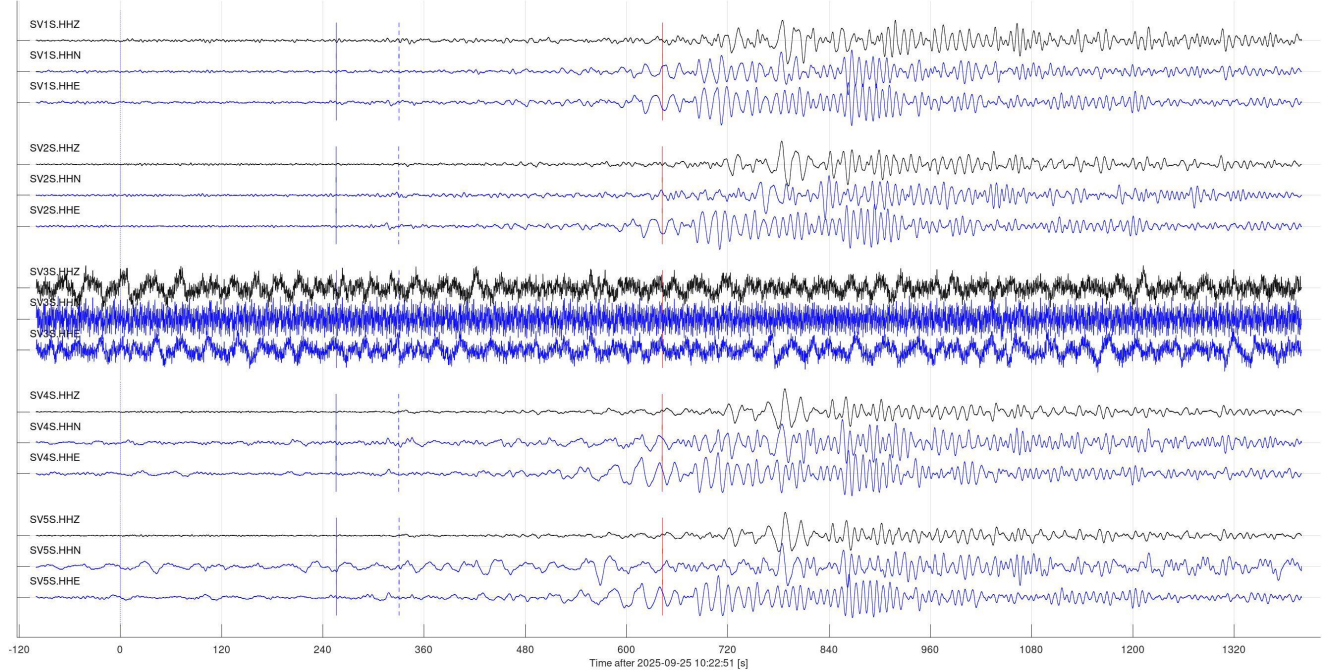


Figure 6, continued.

Event 30708 (us6000rcrj, us): mb 5.8; 2025-09-25 06:55:39 9.89N, 70.67W: 28 km E of Mene Grande, Venezuela
 $V_p=10.00$ km/s; $V_s=5.77$ km/s; $\text{baz}=134.3$ deg; $\text{dist}=47.5$ deg; $\text{depth}=10$ km

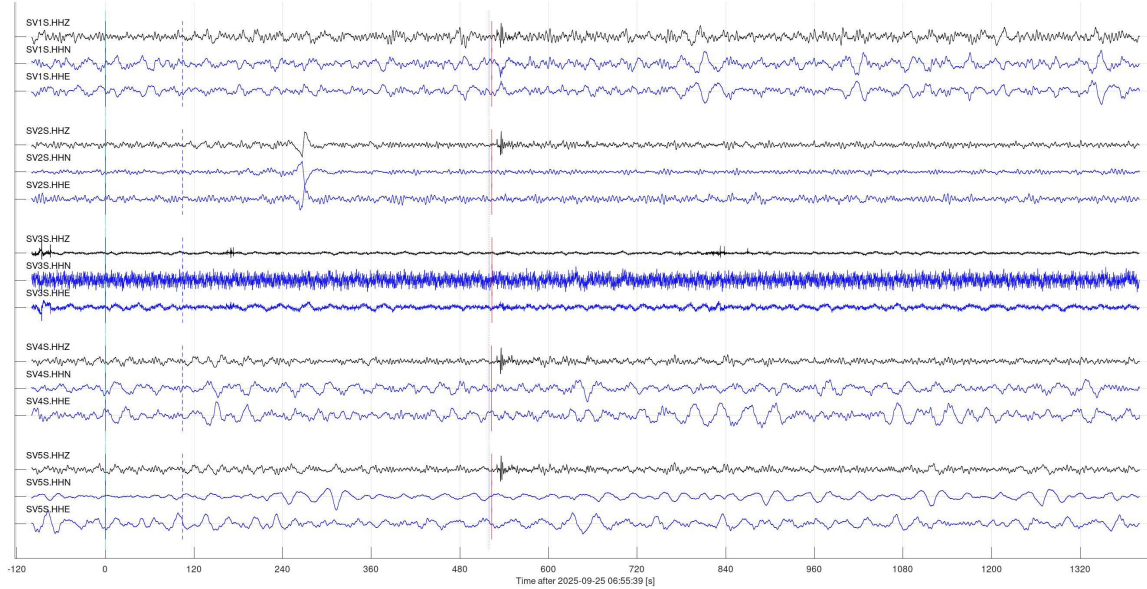


Figure 6, continued.

Event 30783 (us6000rdd9, us): mww 5.1; 2025-09-27 22:12:50 43.46N,127.14W: 225 km W of Bandon, Oregon
 $V_p=10.00$ km/s; $V_s=5.77$ km/s; $\text{baz}=260.3$ deg; $\text{dist}=17.5$ deg; depth=10 km

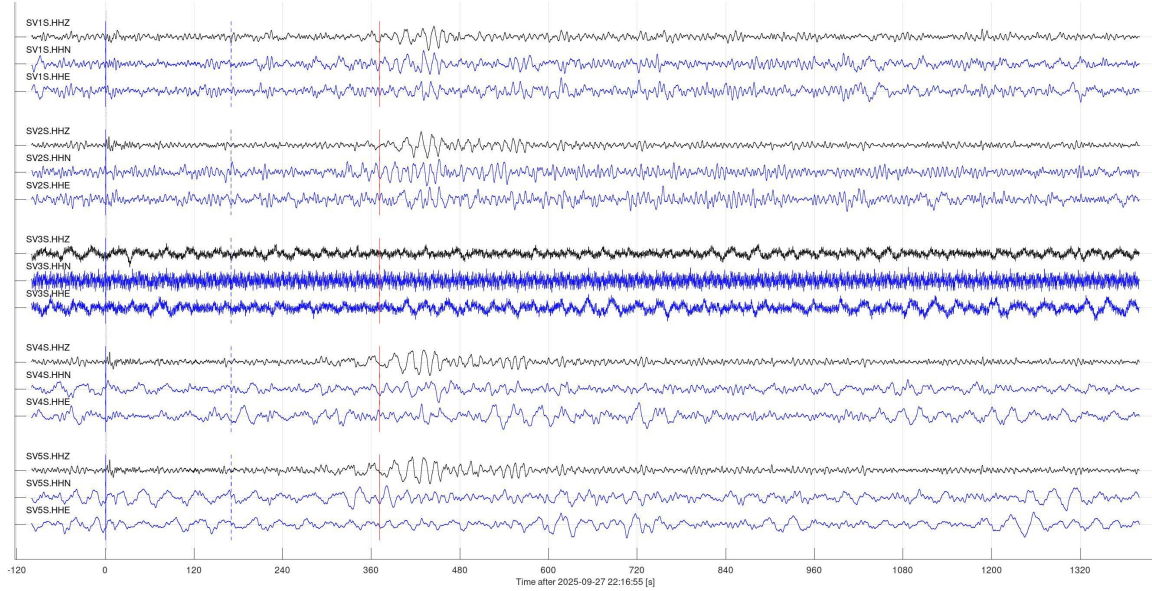


Figure 6, continued.

Event 30804 (us6000rdnq, us): mww 5.5; 2025-09-29 22:07:24 52.92N,159.99E: 92 km E of Petropavlovsk-Kamchatsky, Russia
 $V_p=10.00$ km/s; $V_s=5.77$ km/s; $\text{baz}=313.9$ deg; $\text{dist}=56.5$ deg; depth=42 km

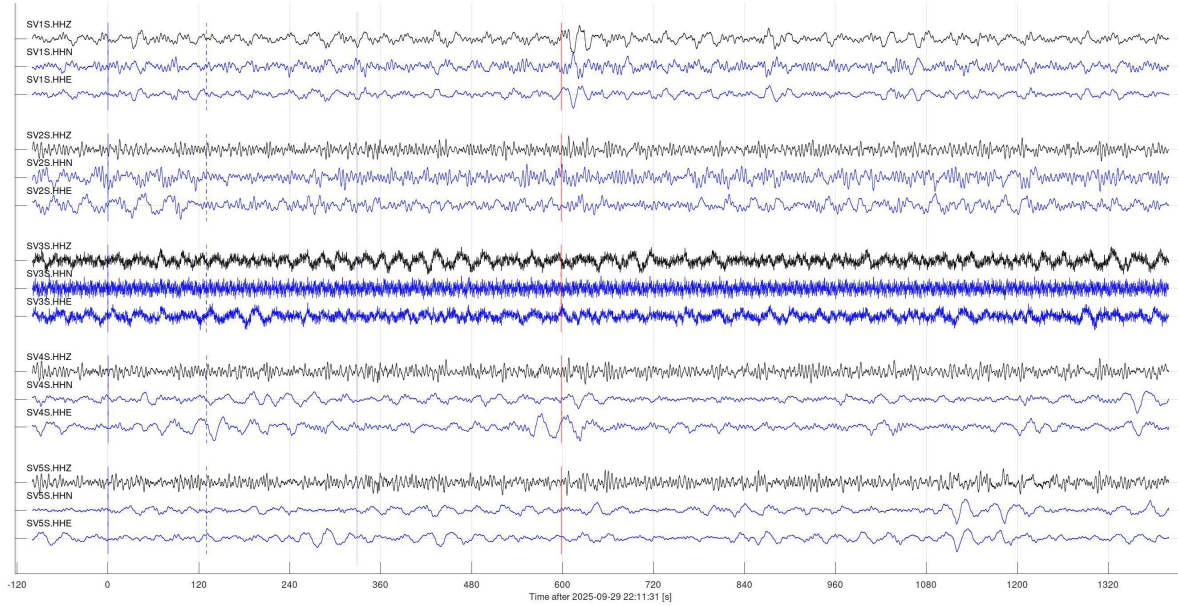


Figure 6, continued.

Event 30932 (us6000drz, us): mww 6.9; 2025-09-30 13:59:43 11.14N,124.13E: 10 km E of Bateria, Philippines
 $V_p=10.00$ km/s; $V_s=5.77$ km/s; $\text{baz}=311.1$ deg; $\text{dist}=107.1$ deg; $\text{depth}=10$ km

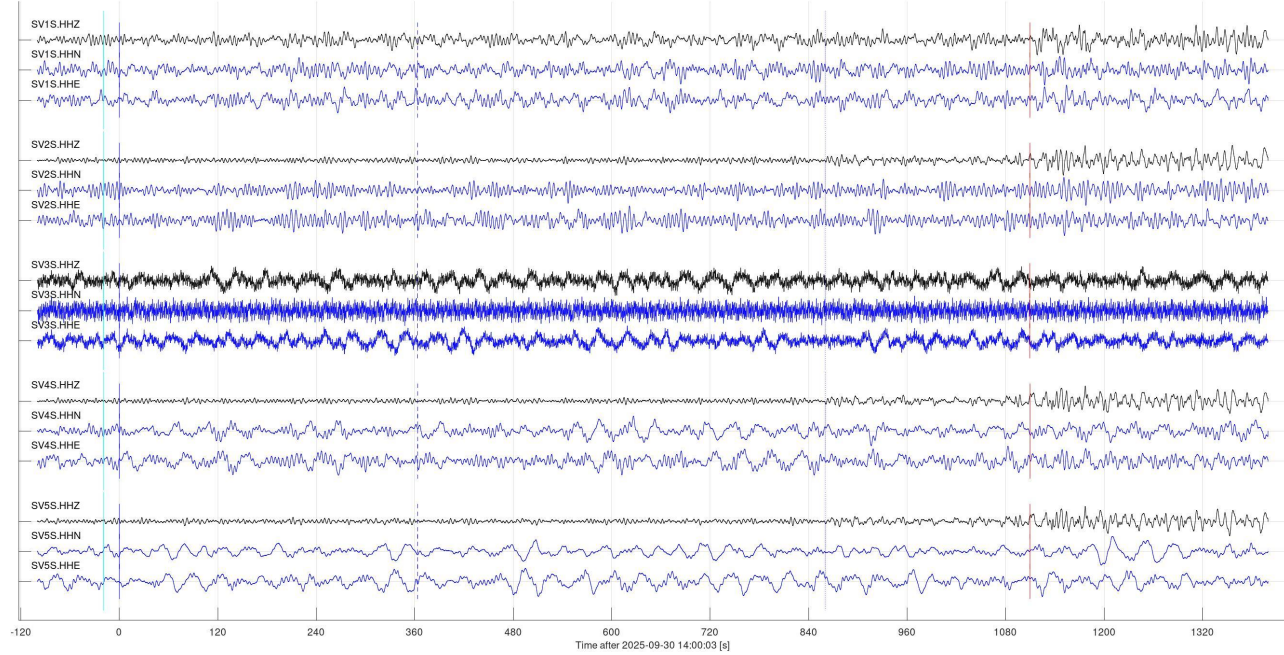


Figure 6, continued.

Regional events (class 2)

No uncatalogued regional seismic events (class 2 in Table 2) were identified in the reporting period.

Local events (classes 3 and 4)

The following subsections summarize observations of event classes 3 and 4 in Table 2.

Possible mine blasts at the Estevan mine (class 3a)

17 detected events were identified as mine blasts in the area of Estevan coal mining (Figure 7). From these events, local P- and S-wave velocities, distances, and back-azimuths were roughly estimated. Locations of some of these events need to be revisited. More accurate location work is in progress.

Event 34204 at 2025-09-05 22:07:50, 'Local': Possible mine blast near Estevan, SK
 $V_p=5.40$ km/s; $V_s=2.80$ km/s; $\text{baz}=90.0$ deg; $\text{dist}=12.0$ km; $\text{depth}=0.00$ km

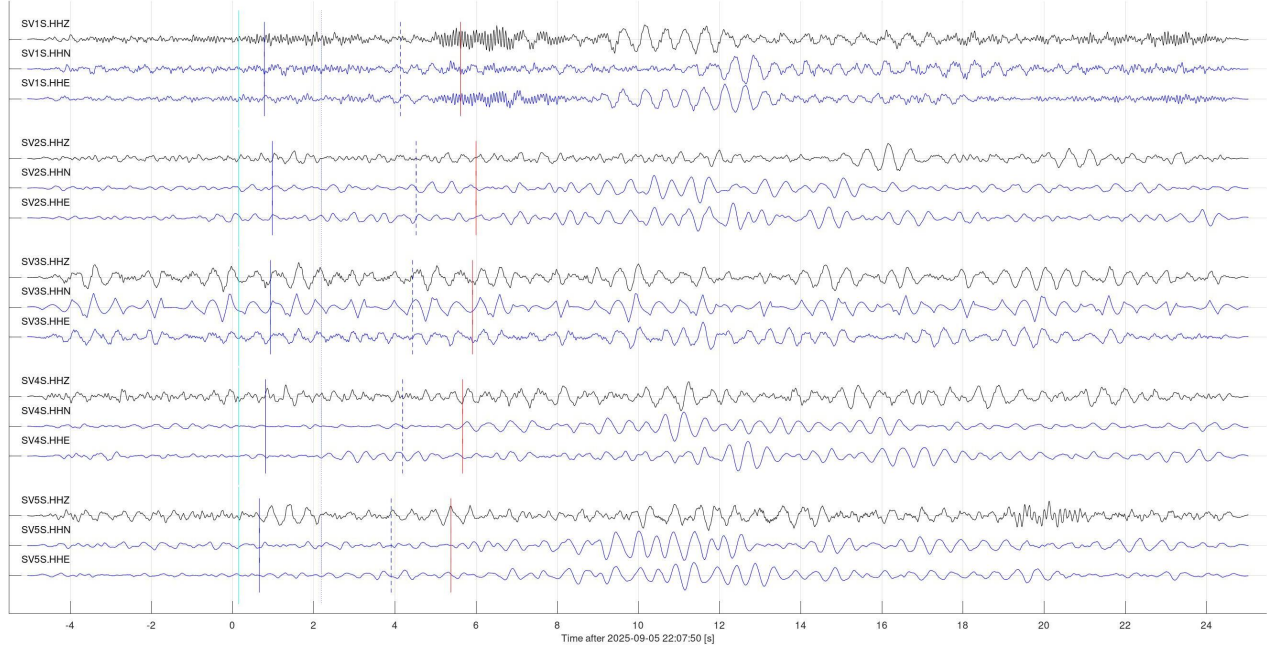


Figure 7. Seismic arrivals produced by mine blasts at the Estevan mine. Colours and labels are as in Figure 6.

Event 34206 at 2025-09-07 20:59:13, 'Local': Possible mine blast near Estevan, SK
 $V_p=5.40$ km/s; $V_s=2.80$ km/s; $\text{baz}=90.0$ deg; $\text{dist}=12.0$ km; $\text{depth}=0.00$ km

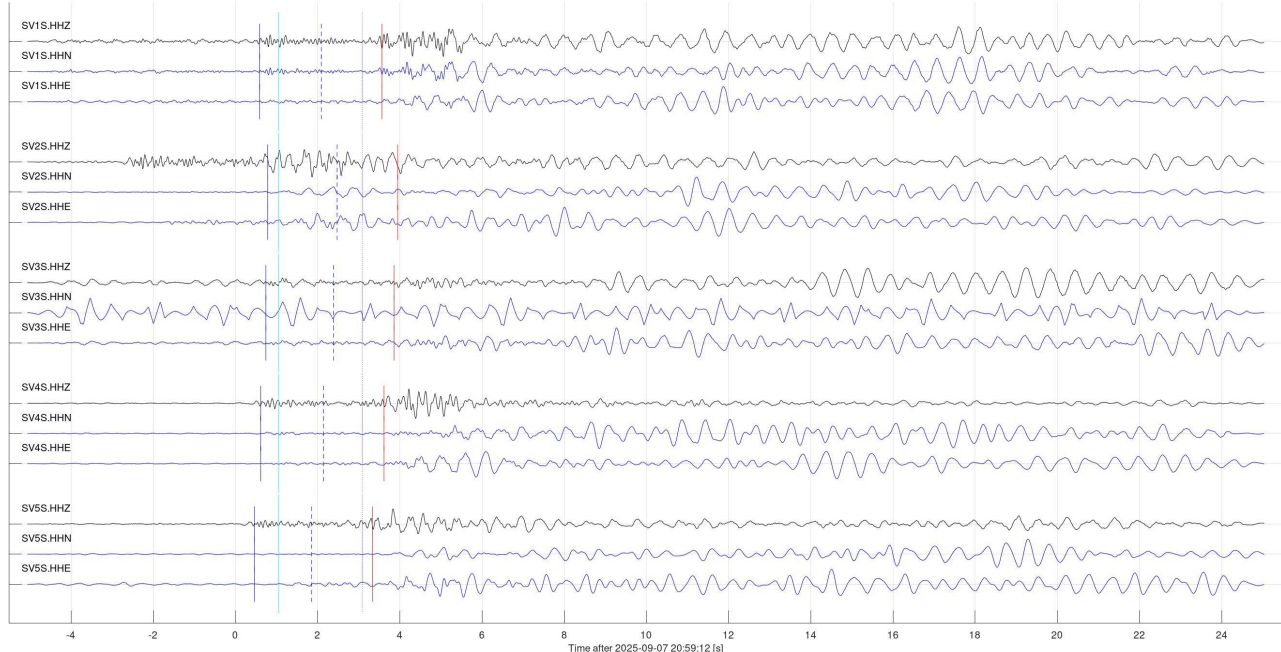


Figure 7, continued.

Event 34208 at 2025-09-09 21:31:49, 'Local': Possible mine blast near Estevan, SK
 $V_p=5.40 \text{ km/s}$; $V_s=2.80 \text{ km/s}$; $\text{baz}=90.0 \text{ deg}$; $\text{dist}=12.0 \text{ km}$; $\text{depth}=0.00 \text{ km}$

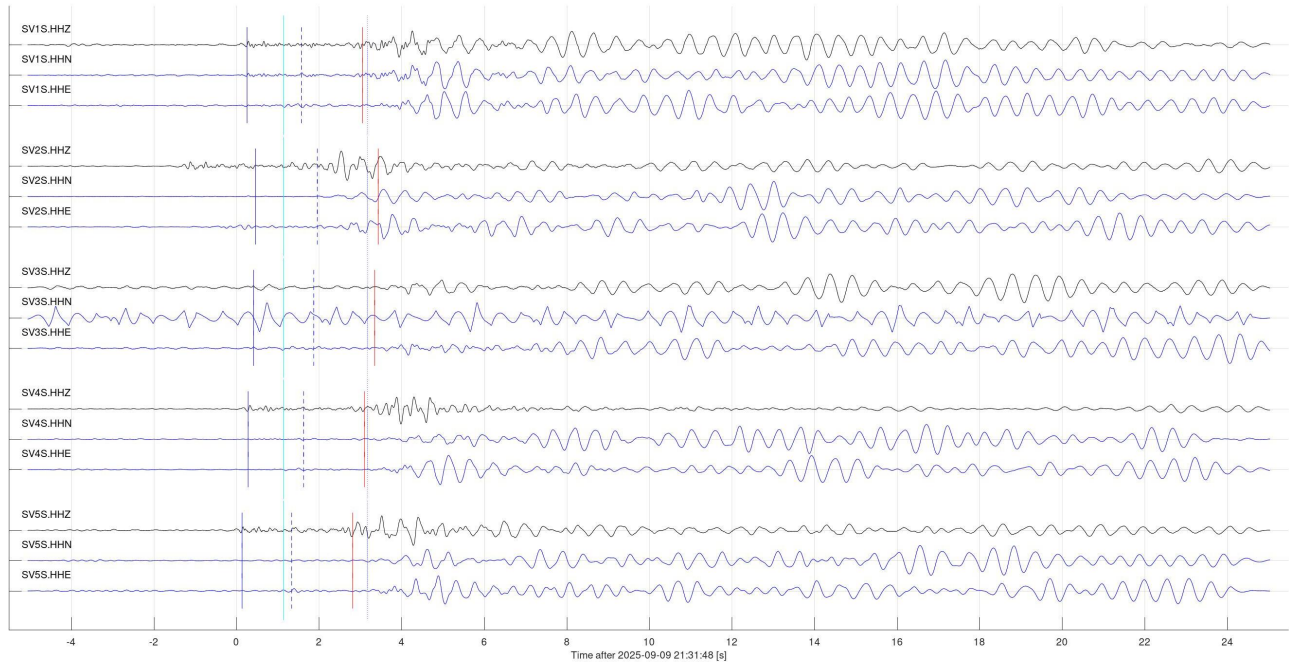


Figure 7, continued.

Event 34357 at 2025-09-10 19:17:33, 'Local': Weaker mine blast?
 $V_p=5.40 \text{ km/s}$; $V_s=2.80 \text{ km/s}$; $\text{baz}=90.0 \text{ deg}$; $\text{dist}=12.0 \text{ km}$; $\text{depth}=0.00 \text{ km}$

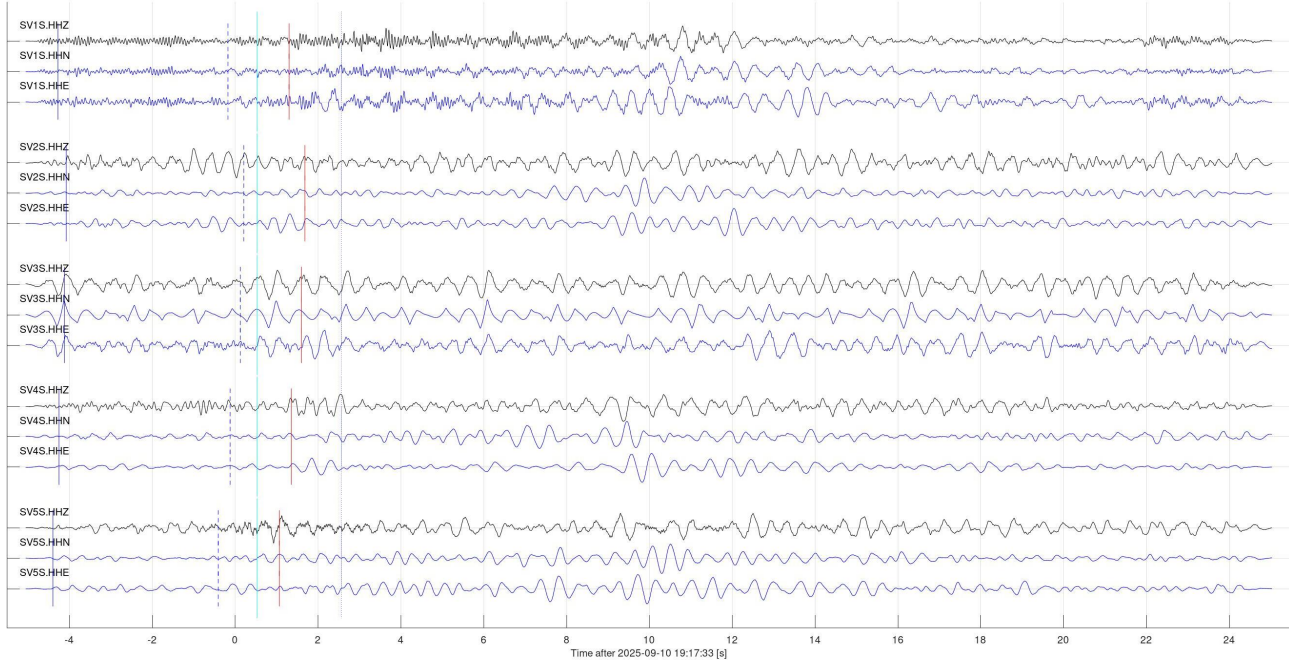


Figure 7, continued.

Event 34359 at 2025-09-10 21:37:43, 'Local': Possible mine blast near Estevan, SK
 $V_p=5.40 \text{ km/s}$; $V_s=2.80 \text{ km/s}$; $\text{baz}=90.0 \text{ deg}$; $\text{dist}=12.0 \text{ km}$; $\text{depth}=0.00 \text{ km}$

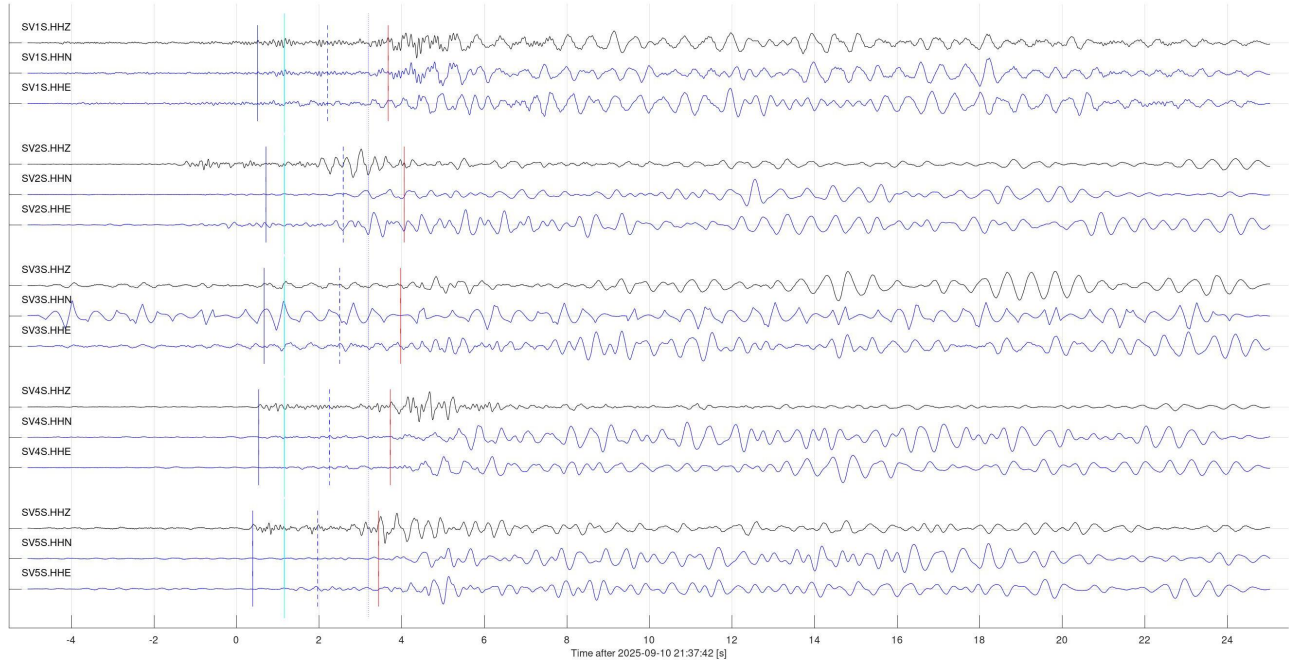


Figure 7, continued.

Event 34360 at 2025-09-12 20:32:31, 'Local': Possible mine blast near Estevan, SK
 $V_p=5.40 \text{ km/s}$; $V_s=2.80 \text{ km/s}$; $\text{baz}=90.0 \text{ deg}$; $\text{dist}=12.0 \text{ km}$; $\text{depth}=0.00 \text{ km}$

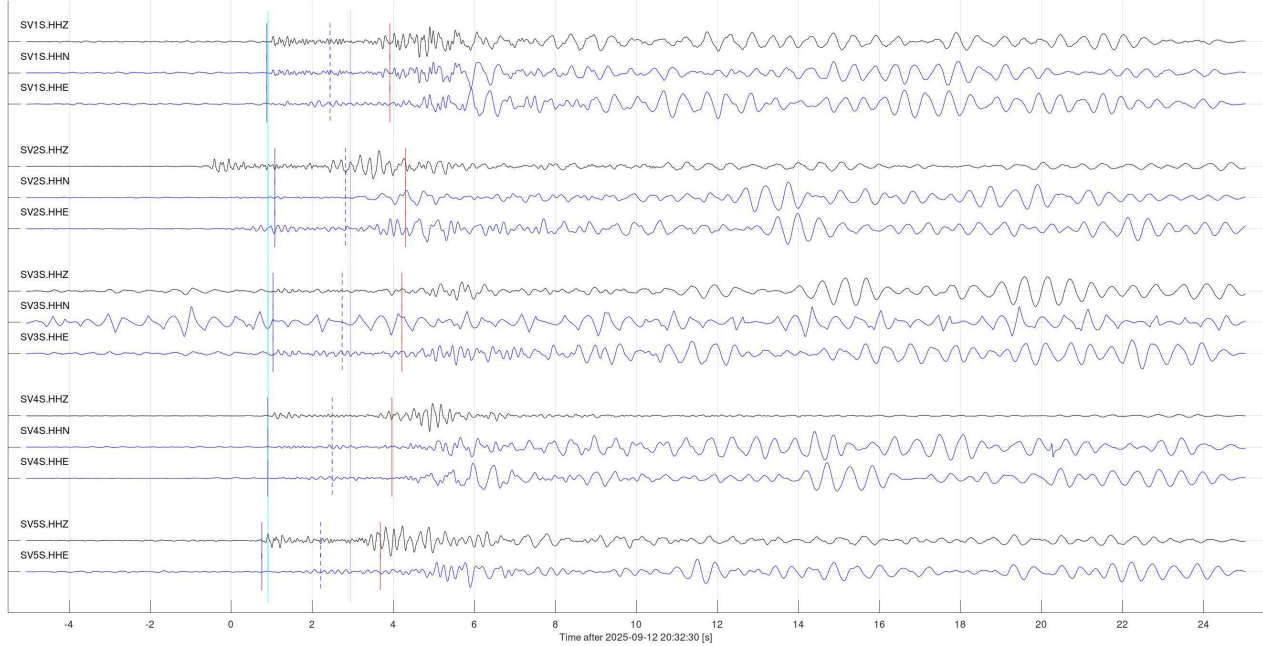


Figure 7, continued.

Event 34362 at 2025-09-17 21:18:12, 'Local': Possible mine blast near Estevan, SK
 $V_p=5.40 \text{ km/s}$; $V_s=2.80 \text{ km/s}$; $\text{baz}=90.0 \text{ deg}$; $\text{dist}=12.0 \text{ km}$; $\text{depth}=0.00 \text{ km}$

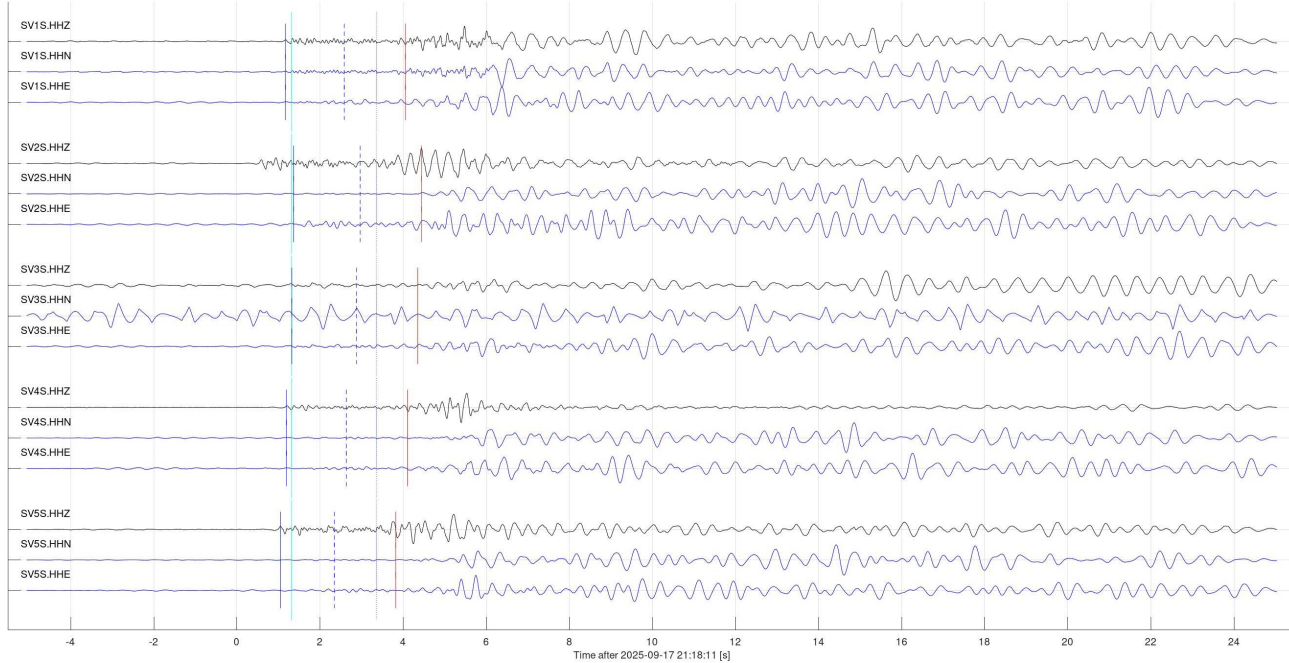


Figure 7, continued.

Event 34363 at 2025-09-19 21:32:42, 'Local': Possible mine blast near Estevan, SK
 $V_p=5.40 \text{ km/s}$; $V_s=2.80 \text{ km/s}$; $\text{baz}=90.0 \text{ deg}$; $\text{dist}=12.0 \text{ km}$; $\text{depth}=0.00 \text{ km}$

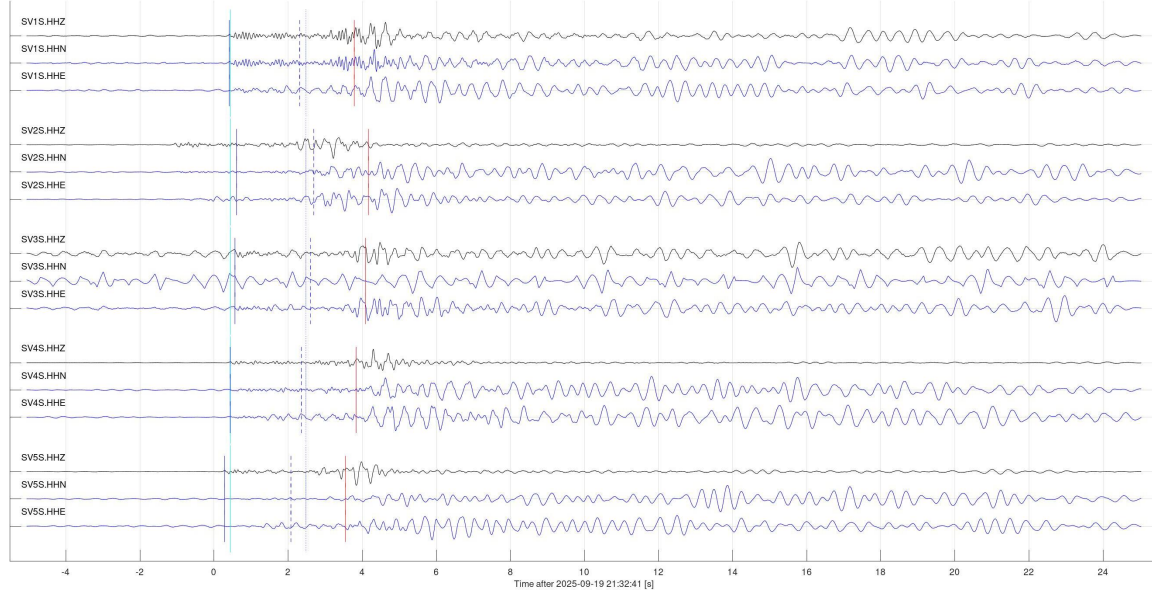


Figure 7, continued.

Event 34364 at 2025-09-20 21:09:18, 'Local': Possible mine blast near Estevan, SK
 $V_p=5.40 \text{ km/s}$; $V_s=2.80 \text{ km/s}$; $\text{baz}=90.0 \text{ deg}$; $\text{dist}=12.0 \text{ km}$; $\text{depth}=0.00 \text{ km}$

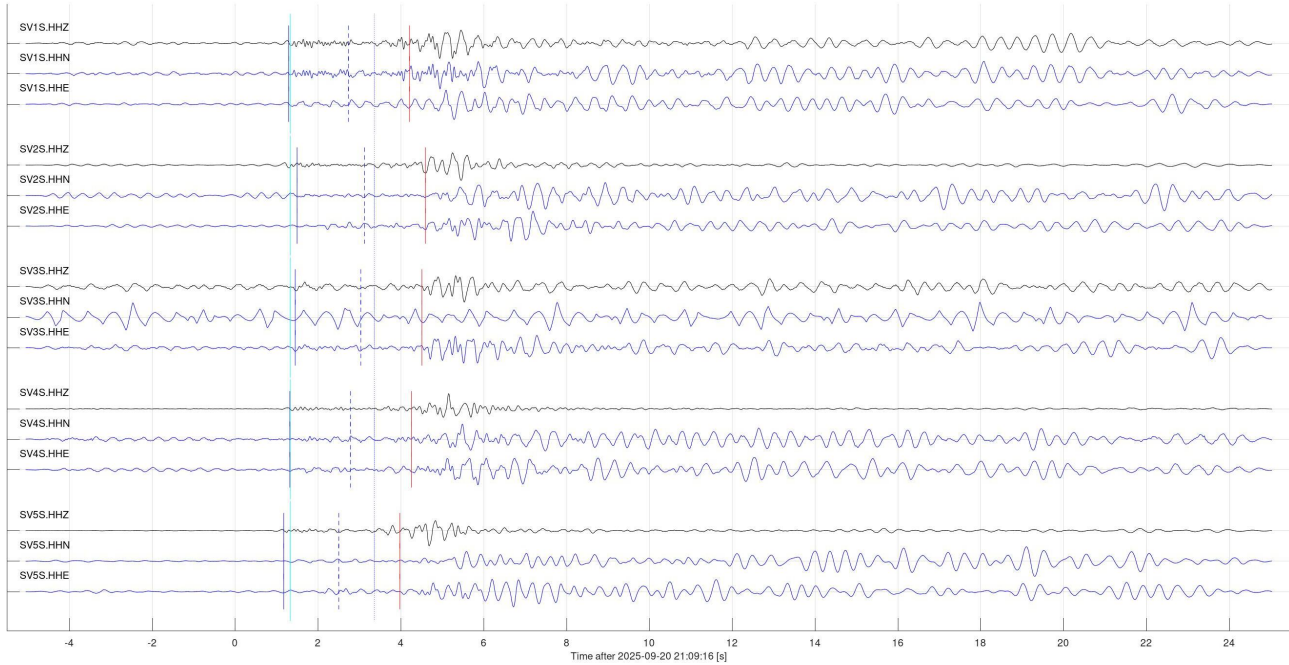


Figure 7, continued.

Event 34365 at 2025-09-21 20:50:20, 'Local': Possible mine blast near Estevan, SK
 $V_p=5.40 \text{ km/s}$; $V_s=2.80 \text{ km/s}$; $\text{baz}=90.0 \text{ deg}$; $\text{dist}=12.0 \text{ km}$; $\text{depth}=0.00 \text{ km}$

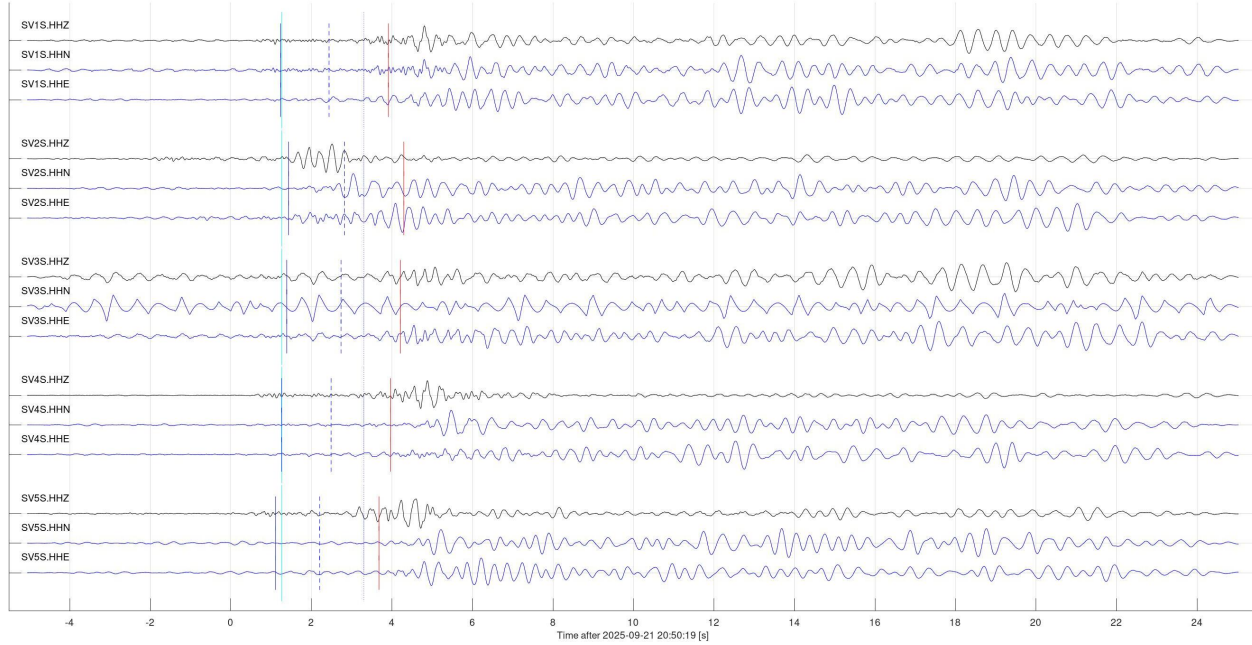


Figure 7, continued.

Event 34366 at 2025-09-22 21:12:10, 'Local': Possible mine blast near Estevan, SK
 $V_p=5.40 \text{ km/s}$; $V_s=2.80 \text{ km/s}$; $\text{baz}=90.0 \text{ deg}$; $\text{dist}=12.0 \text{ km}$; $\text{depth}=0.00 \text{ km}$

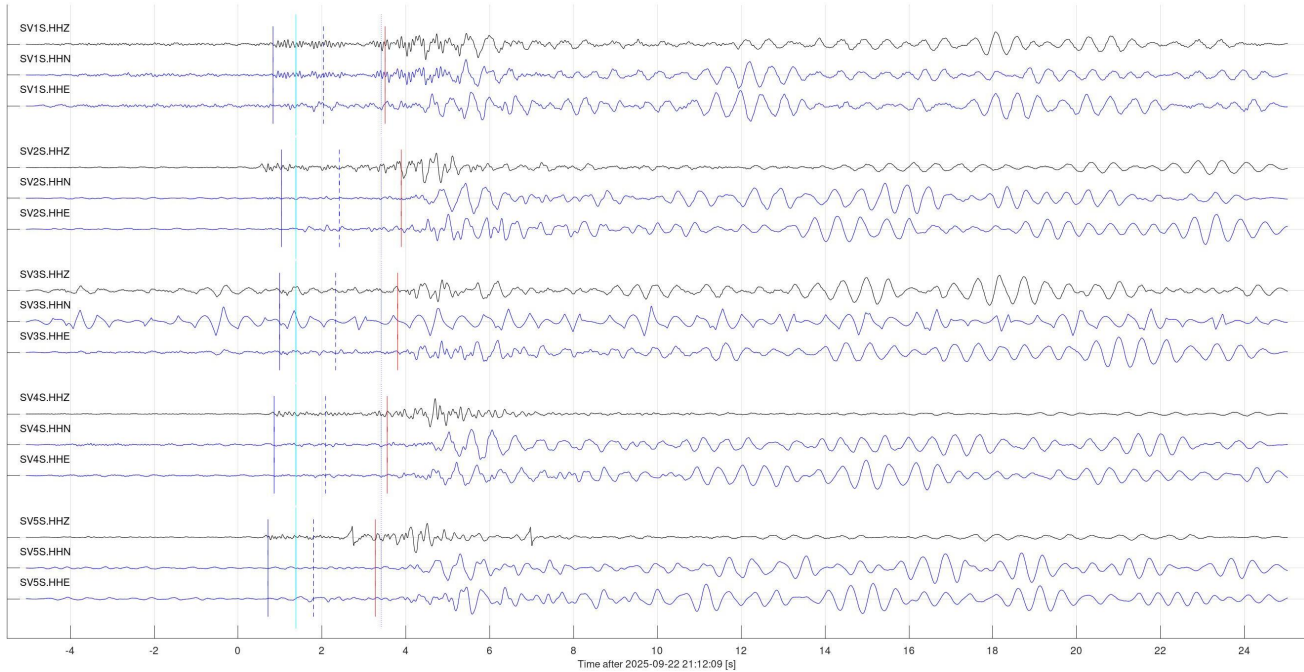


Figure 7, continued.

Event 34367 at 2025-09-24 21:33:44, 'Local': Possible mine blast near Estevan, SK
 $V_p=5.40 \text{ km/s}$; $V_s=2.80 \text{ km/s}$; $\text{baz}=90.0 \text{ deg}$; $\text{dist}=12.0 \text{ km}$; $\text{depth}=0.00 \text{ km}$

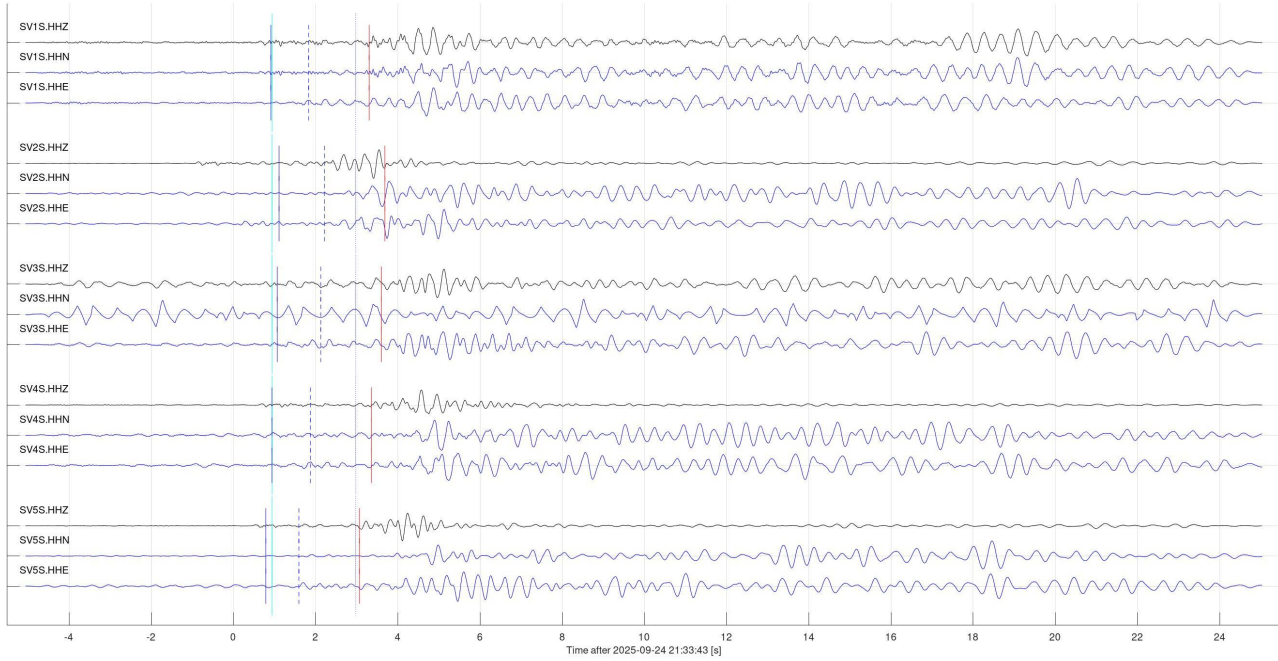


Figure 7, continued.

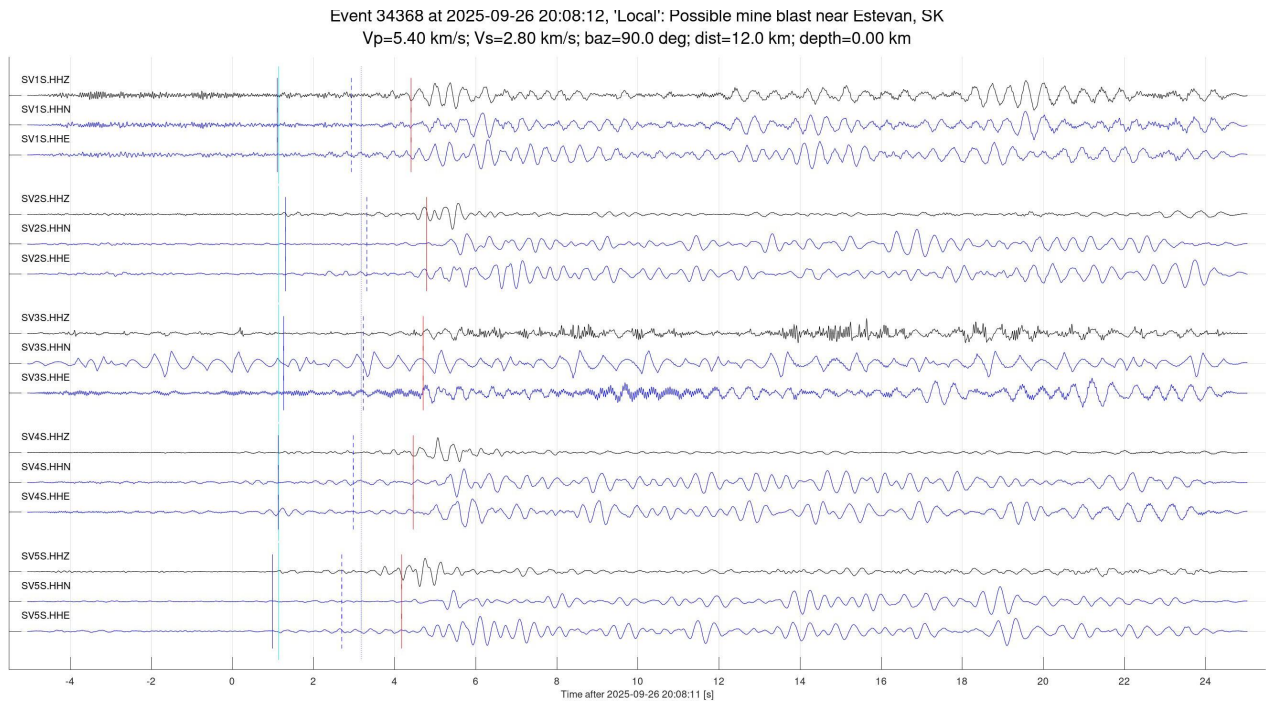


Figure 7, continued.

Event 34369 at 2025-09-27 21:36:29, 'Local': Possible mine blast near Estevan, SK
 $V_p=5.40 \text{ km/s}$; $V_s=2.80 \text{ km/s}$; $\text{baz}=90.0 \text{ deg}$; $\text{dist}=12.0 \text{ km}$; $\text{depth}=0.00 \text{ km}$

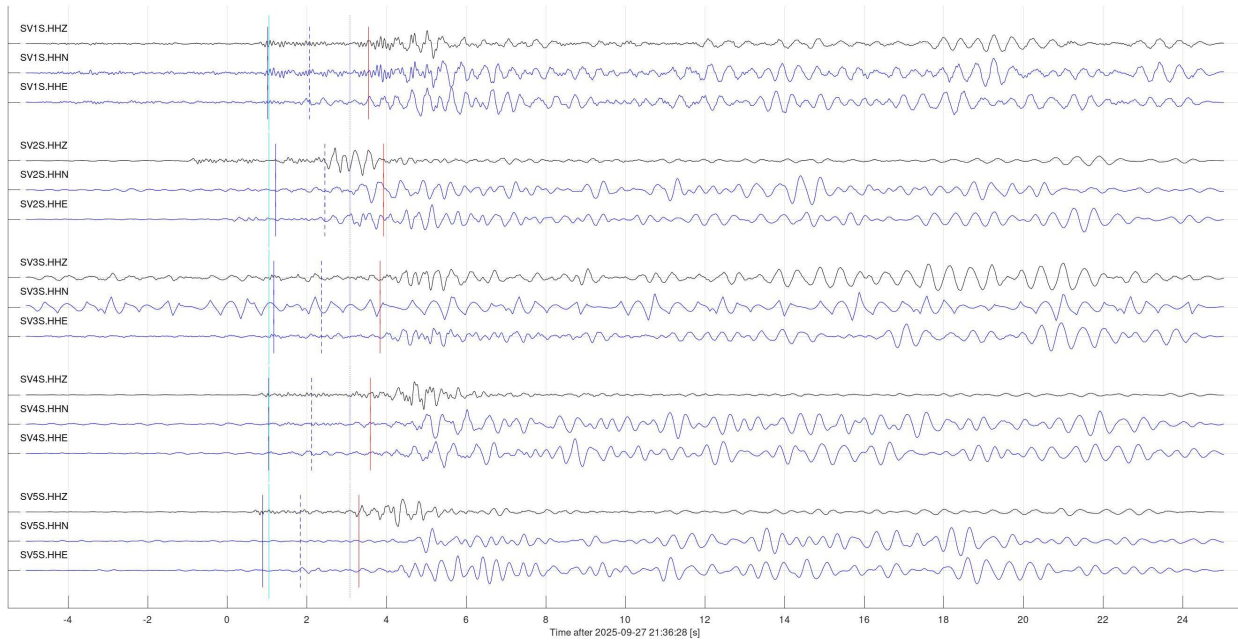


Figure 7, continued.

Event 34370 at 2025-09-28 21:39:10, 'Local': Possible mine blast near Estevan, SK
 $V_p=5.40 \text{ km/s}$; $V_s=2.80 \text{ km/s}$; $\text{baz}=90.0 \text{ deg}$; $\text{dist}=12.0 \text{ km}$; $\text{depth}=0.00 \text{ km}$

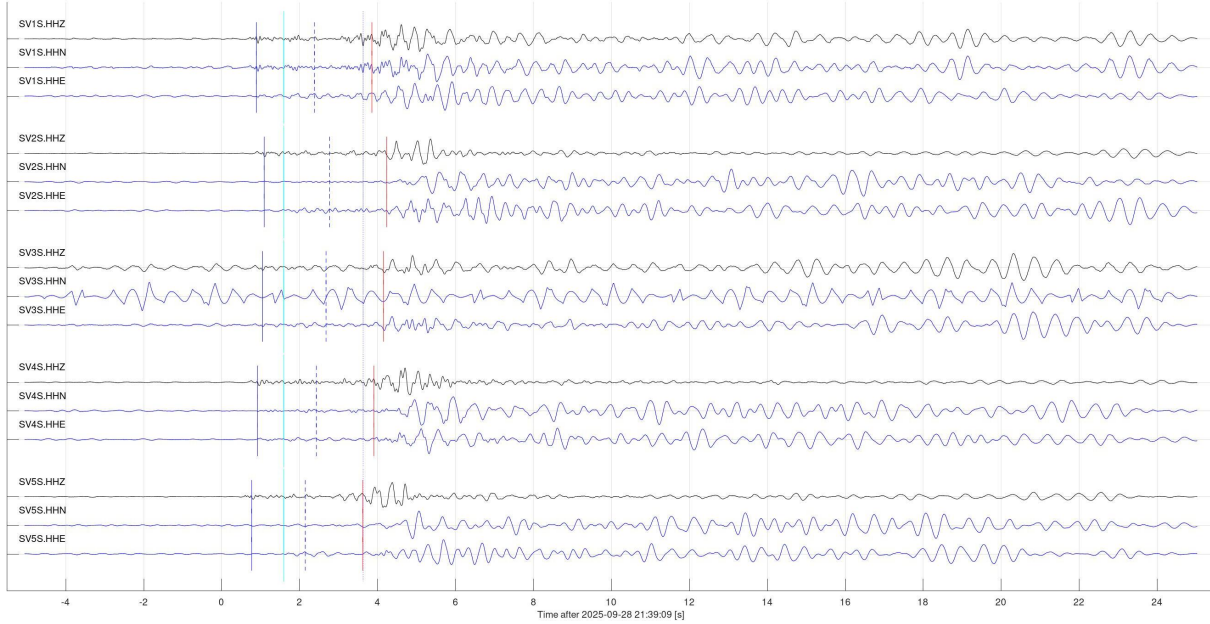


Figure 7, continued.

Event 34371 at 2025-09-29 21:41:35, 'Local': Possible mine blast near Estevan, SK
 $V_p=5.40$ km/s; $V_s=2.80$ km/s; $\text{baz}=90.0$ deg; $\text{dist}=12.0$ km; depth=0.00 km

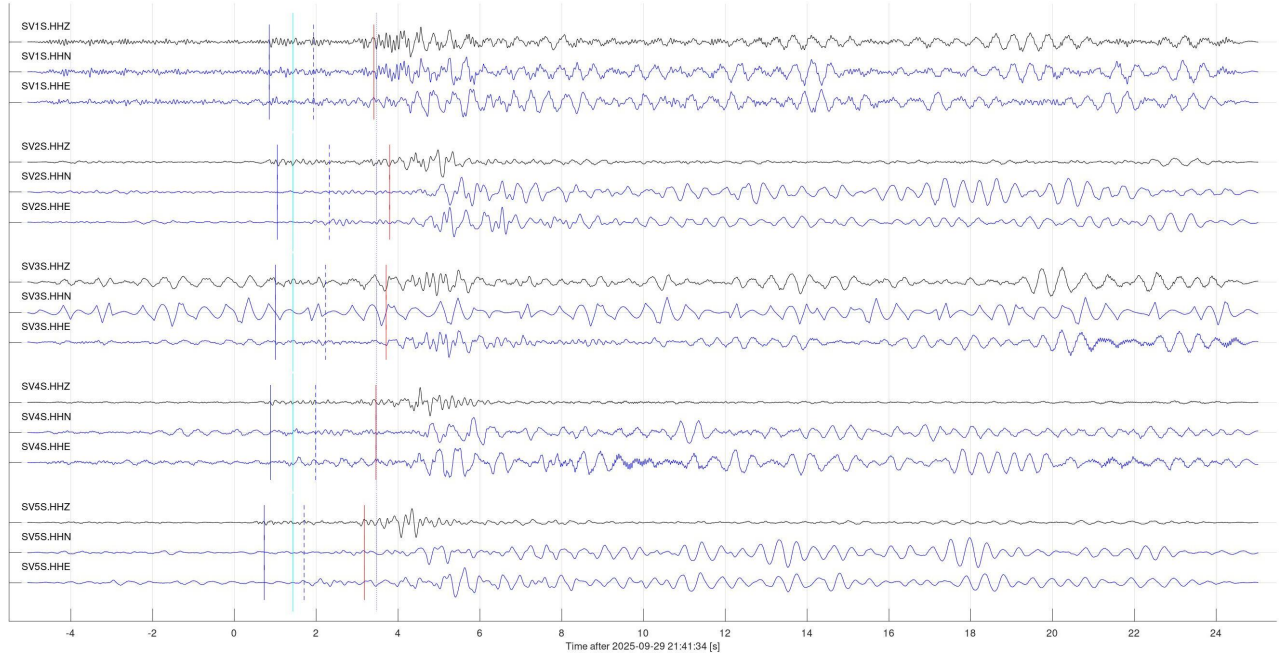


Figure 7, continued.

Event 34372 at 2025-09-30 21:08:24, 'Local': Possible mine blast near Estevan, SK
 $V_p=5.40$ km/s; $V_s=2.80$ km/s; $\text{baz}=90.0$ deg; $\text{dist}=12.0$ km; depth=0.00 km

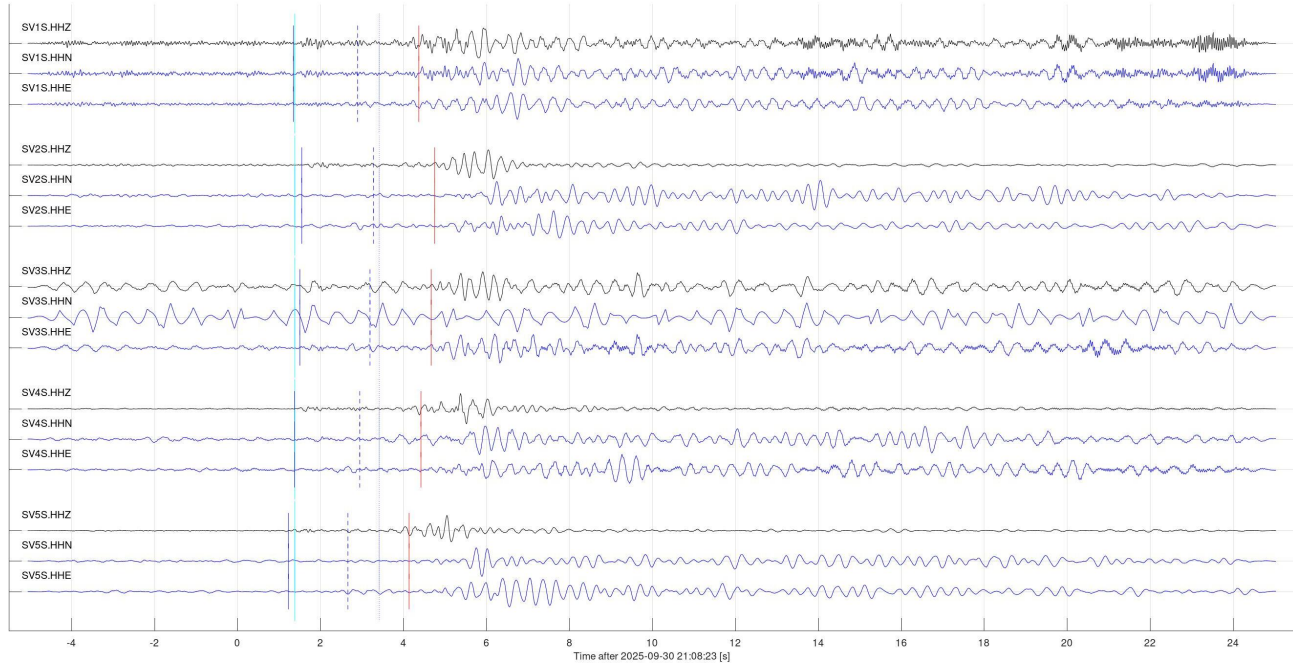


Figure 7, continued.

Events related to mining operations (class 3b)

Numerous mining- and industrial-operations related seismic events were observed in the area. Figure 8 illustrates two of them, arbitrarily selected as appearing worth returning to later. Some of them (longer waveforms with strongly pronounced and lower dominant frequencies) may be produced by trains.

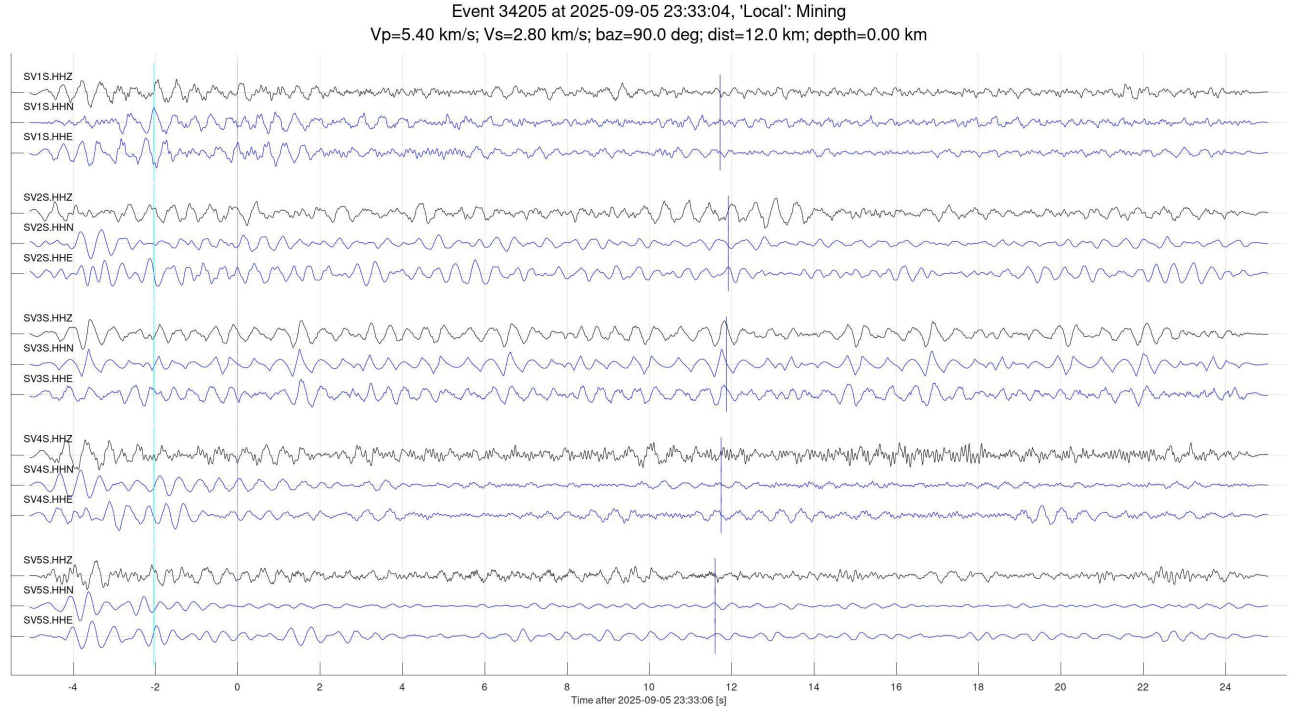


Figure 8. Sample events interpreted as due to mining activity in the area. Lines, color bars and labels are as in the preceding figures.

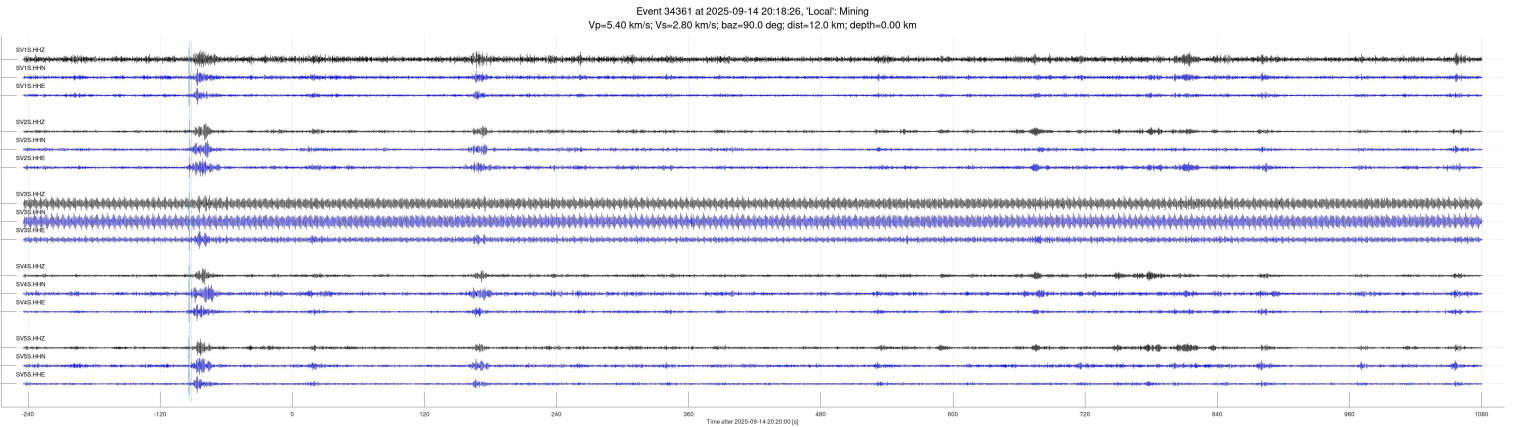


Figure 8, continued (longer time interval shown).

Events in array proximity (classes 4a and 4b)

Three groups of seismic events were identified as possibly occurring in the proximity of the array (class 4a) (Figure 9). All of these events likely originate in the near surface, which is suggested by strong differences in frequency content and large travel-time moveouts. With only four or five available stations, it is difficult to determine the depths of potential events and differentiate between classes 4a and 4b.

An interesting peculiarity of this month's near-array, near-surface events in appearances of long series of about 20 or more sharp strikes separated by a relatively consistent 100 to 120-s intervals (last two panels of Figure 9). This pattern appears to be different from what is usually seen from trains. Apparently, this type of seismic noise could be produced by mining or excavation operations near the Aquistore area.

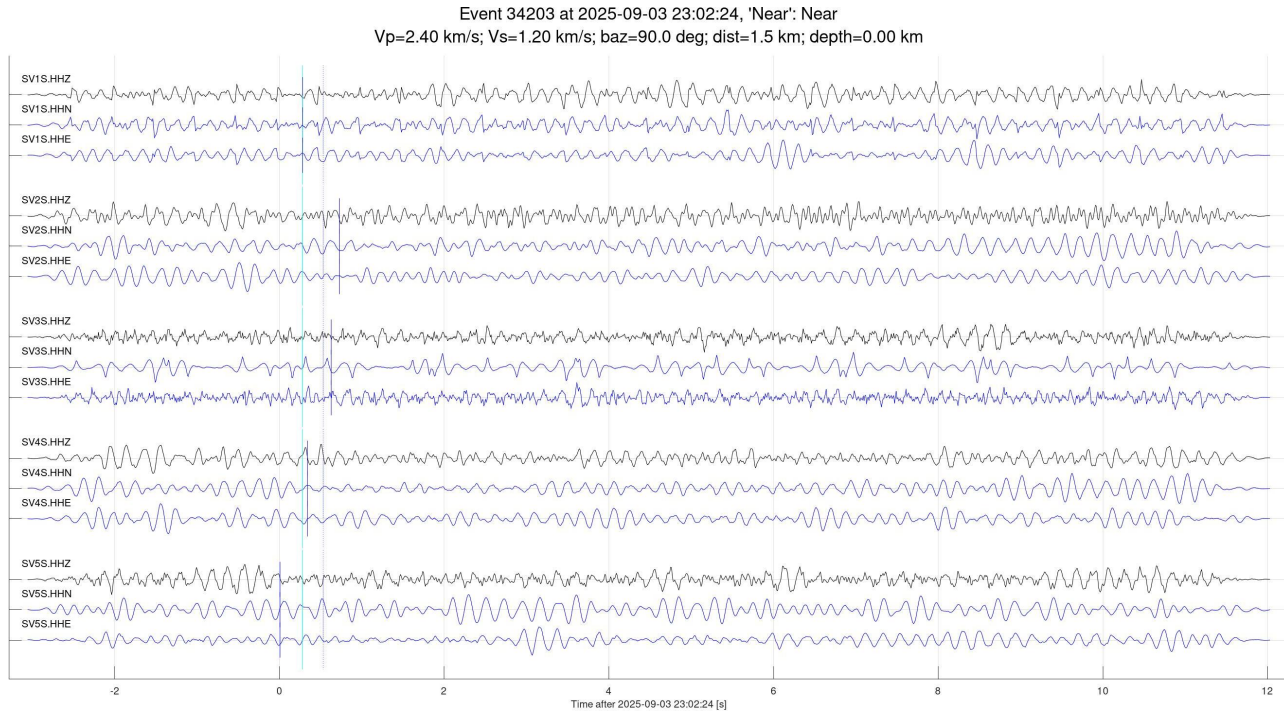


Figure 9. Events interpreted as occurring near surface in the proximity of the array (class 4a in Table 2). Lines, colour bars and labels are as in the preceding figures.

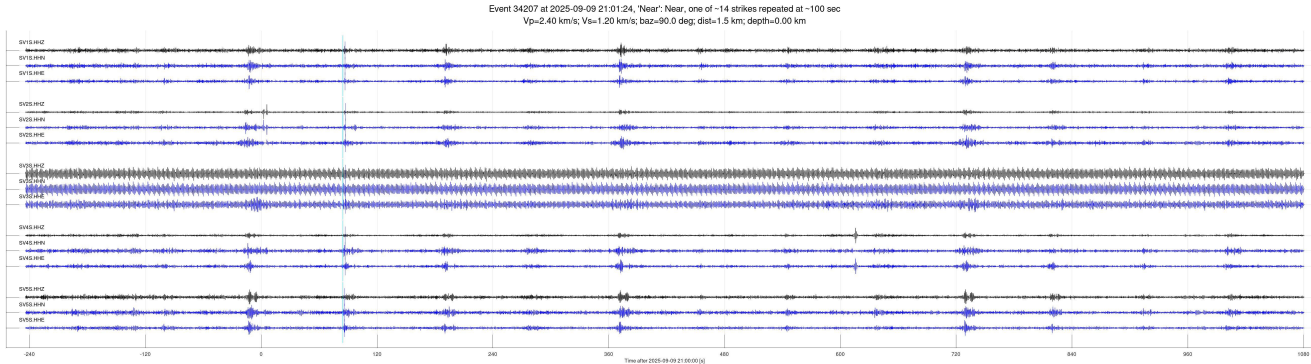


Figure 9, continued. This and the following images illustrate long series of up to about 20 events repeated at about 100-s intervals

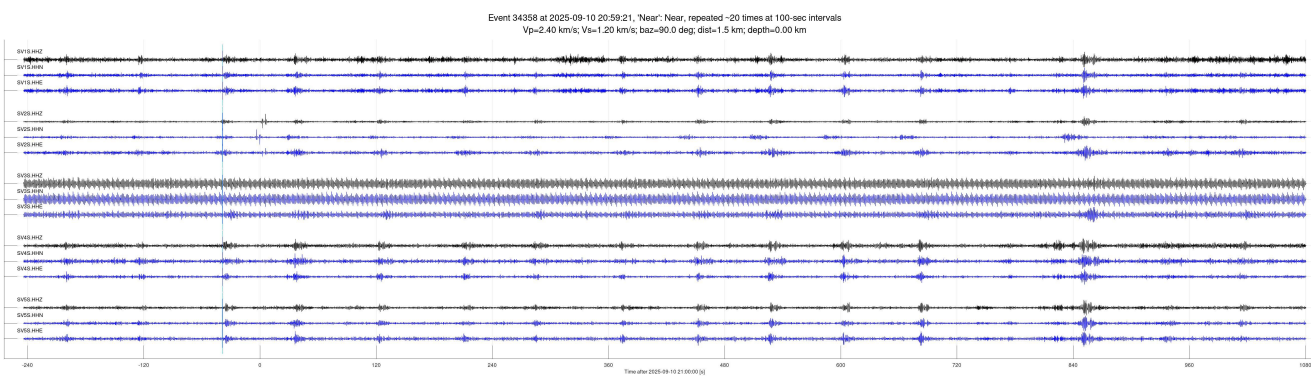


Figure 9, continued.

5. SEGY files

Event time windows are provided in SEGY format in the attached zipped archive, separately for teleseismic and regional event detections. Subdirectory names and file naming convention and header formats are described in our reports for August and October 2024.

6. Conclusions and recommendations

- Major maintenance operations were completed in September 2025:
 - Cell internet service was switched to a different provider (SaskTel Fusion) and new modems were sourced and installed;
 - Cause of malfunctioning of station SV3S was identified (sensor cable) and a new cable ordered from Nanometrics.
- With the exceptions of station SV3S for weaker signals and channel SV5S.HNE, the Aquistore broadband seismic array operated well.

- 26 strong telesismic events and 17 mine blasts were detected in September 2025.
- Numerous local events were detected, likely related to mining operations or freight trains. These events were not catalogued or analyzed in detail.
- Several examples of near-surface seismic activity in the vicinity of the array were noted, including an apparently new one with repetitive sharp striking at the surface. No events occurring at the reservoir level were identified.